simultaneously inhibit Notch activation and promote differentiation to goblet cells in the mice intestine.

We also found marked atrophy of the thymus in LY411,575-treated mice (Supplemental Fig. S1*A*). Supplemental data for this article are available on the *American Journal of Physiology Gastrointestinal and Liver Physiology* website. Further analysis of the thymus revealed that the total number of thymocytes was significantly reduced (Supplemental Fig. S1*B*) and that the tissue architecture was disrupted (Supplemental Fig. S1*C*). Analysis of CD4/CD8 expression revealed a significant proportional reduction in double-positive cells (Supplemental Fig. S1*D*) and a reduction in the absolute number of cells (Supplemental Fig. S1*E*), suggesting that there was a significant loss of immature cells in the thymus with LY411,575 treatment. However, such an effect of LY411,575 was not present in the spleen (Supplemental Fig. S1, *A–E*). These findings clearly showed that the LY411,575 treatment had a systemic effect, affecting the thymus in addition to the intestine.

LY411,575 exacerbates DSS-colitis by impairing epithelial regeneration. Using the methods described, we designed an experiment to examine the effect of Notch inhibition during colitis (Fig. 2*B*). Mice were separated into four groups: vehicle alone (VEC), LY411,575 alone (LY), DSS with vehicle (DSS + VEC), and DSS with LY411,575 (DSS + LY). As of *day 5*, the total body weights showed significant reductions from *day 0* in DSS-treated mice (Fig. 2*B*) compared with the weights of those without DSS (the day when DSS treatment was started is designated as *day 0*). However, the DSS + LY mice showed even greater reductions in weight as of *day 8*; their reductions in body weight were significantly greater than the weight reductions in DSS + VEC mice (Fig. 2*B*). This severe loss of body weight observed in DSS + LY mice was also fatal because two mice in this group were dead at the time of euthanasia (fatality rate = 2/6, 33.3%). No deaths were observed in any other experimental group. These results suggested that LY411,575 significantly exacerbates the clinical course of DSS-colitis. A histological analysis of LY or DSS + LY mice showed a marked increase in goblet cells in the small intestine, confirming the effect of LY411,575 treatment (Fig. 2*C*). The increase in goblet cells was also observed in the colon of LY mice. A histological analysis of DSS + VEC mice showed a clear induction of colitis, as shown by the marked increase in inflammatory cells and the elongation of goblet cell depleted crypts. However, in sharp contrast, DSS + LY mice showed a severe loss of the epithelial layer in addition to an infiltration of inflammatory cells, which appeared to lack signs of epithelial regeneration (Fig. 2*C*). A histological scoring of the colonic tissues revealed increased ulcer formation and epithelial injury in DSS + LY mice compared with DSS + VEC mice, whereas no significant changes were observed in the degree of inflammation (Fig. 2*D*). Consistent with this, the mRNA expression of proinflammatory cytokines was increased in the colon of DSS-treated mice, but no clear differences were observed between DSS + VEC and DSS + LY mice (Supplemental Fig. S2).

For further analysis, we examined the expression of Hes1 and Ki-67 in the inflamed region of the colonic tissues. An increase in Hes1- or Ki-67-positive IECs was confirmed in DSS + VEC mice (Fig. 2*E*). However, both Hes1 and Ki-67 expression appeared to be markedly lost in the colonic crypts upon LY411,575 treatment (Fig. 2*E*). These results indicated that LY411,575 inhibits Notch activation and promotes goblet cell differentiation but also strongly inhibits proliferation of IECs, leading to a poor regenerative response and a severe exacerbation of DSS-colitis.

LY411,575 promotes goblet cell differentiation but inhibits proliferation of IECs in vitro. Previous in vivo results suggested that Notch activation might play critical roles in both the differentiation and proliferation of IECs. We further examined the in vitro effect of LY411,575 upon human colonic epithelial cell lines LS174T and HT29. As shown by the immunoblot analysis, the endogenous expression of both NICD1 and Hes1 was completely inhibited within LS174T cells by LY411,575 treatment (Fig. 3*A*). Consistent with this, RT-PCR analysis showed a marked decrease in Hes1 mRNA expression with LY411,575, which was maintained for up to 72 h (Fig. 3*B*). These data confirmed that LY411,575 could directly inhibit the activation of Notch within IECs.

Under this condition, we examined whether LY411,575 could promote goblet cell differentiation in vitro. Quantitative RT-PCR analysis showed a significant increase in MUC2 mRNA expression with LY411,575 treatment in both LS174T and HT29 cells (Fig. 3*C*). Consistent with this, a marked induction of MUC2 protein expression was observed in both of the cell lines that were treated with LY411,575 (Fig. 3*D*, red signal), resulting in a significant increase in the MUC2-positive cell population (Fig. 3*E*). The Alcian blue staining also showed a marked increase in mucin-producing cells in both cell lines with LY411,575 (Fig. 3*F*, black arrow). However, LY411,575 appeared to inhibit the proliferation of both cell lines since the incorporation of BrdU was significantly downregulated by LY411,575 (Fig. 3*G*). These results collectively showed that LY411,575 could directly inhibit Notch activation in IECs, which might subsequently promote goblet cell differentiation but also inhibit cell proliferation.

Activation of Notch1 suppresses goblet cell phenotype, but upregulates PLA2G2A secretion in human IECs. To further analyze the function of Notch activation in IECs, we gen-

Fig. 2. Inhibition of Notch activation by LY411,575 exacerbates DSS-colitis by impairing epithelial regeneration. *A*: LY411,575 suppresses Hes1 expression but also promotes MUC2 expression in mice intestine. After oral administration of LY411,575 or vehicle alone for 5 consecutive days, the small intestinal tissues of mice were subjected to quantitative RT-PCR analysis. Results from 3 mice in each group. Error bars represent SD. $*P < 0.05$ on the Student's *t*-test. *B*: LY411,575 significantly exacerbated wasting disease caused by DSS. As described in MATERIALS AND METHODS, mice were separated into 4 groups, and the body weight of each mouse was monitored throughout the experimental period. Error bars represent SD. $*P < 0.05$ for the difference between mice that were DSS treated (DSS + VEC and DSS + LY) or not treated (VEC and LY). $**P < 0.05$ for the difference between DSS + VEC and DSS + LY mice on the Student's *t*-test. *C*: LY411,575 exacerbated epithelial injury of DSS-colitis. Intestinal tissues of mice shown in *B* were subjected to histological analysis. Blue staining with Alcian blue represents mucin production (original magnification ×400). *D*: LY411,575 had no significant effect on inflammation of DSS-colitis. Histological scoring of colonic tissues obtained from each mice group is shown. Error bars represent SD. $*P < 0.05$ on the Student's *t*-test. *E*: LY411,575 inhibited proliferation of IECs via downregulation of Notch activity. Colonic tissues of mice were subjected to immunohistochemical staining for Hes1 and Ki-67. A less inflamed region was chosen for analysis of DSS + LY mice because the most inflamed region showed complete loss of the epithelial layer. Note that IECs expressing Hes1 or Ki-67 were confined within a narrow region of the colonic crypt in mice treated with LY411,575 (LY and DSS + LY).

erated a subline of LS174T cells (Tet-On NICD1 cells), in which forced expression of NICD1 could be induced in a tetracycline- or DOX-dependent manner. Immunoblot analysis of Tet-On NICD1 cells showed a clear induction of NICD1 and a subsequent increase in Hes1, with DOX addition (Fig. 4*A*). Consistent with this, the reporter activity of Hes1p-Luc was significantly upregulated with the induction of NICD1 in Tet-On NICD1 cells, indicating that there was an upregulation of the transcriptional activity of the Hes1 gene (Fig. 4*B*). These results confirmed that Tet-On NICD1 cells could express the functional NICD1 protein with DOX addition.

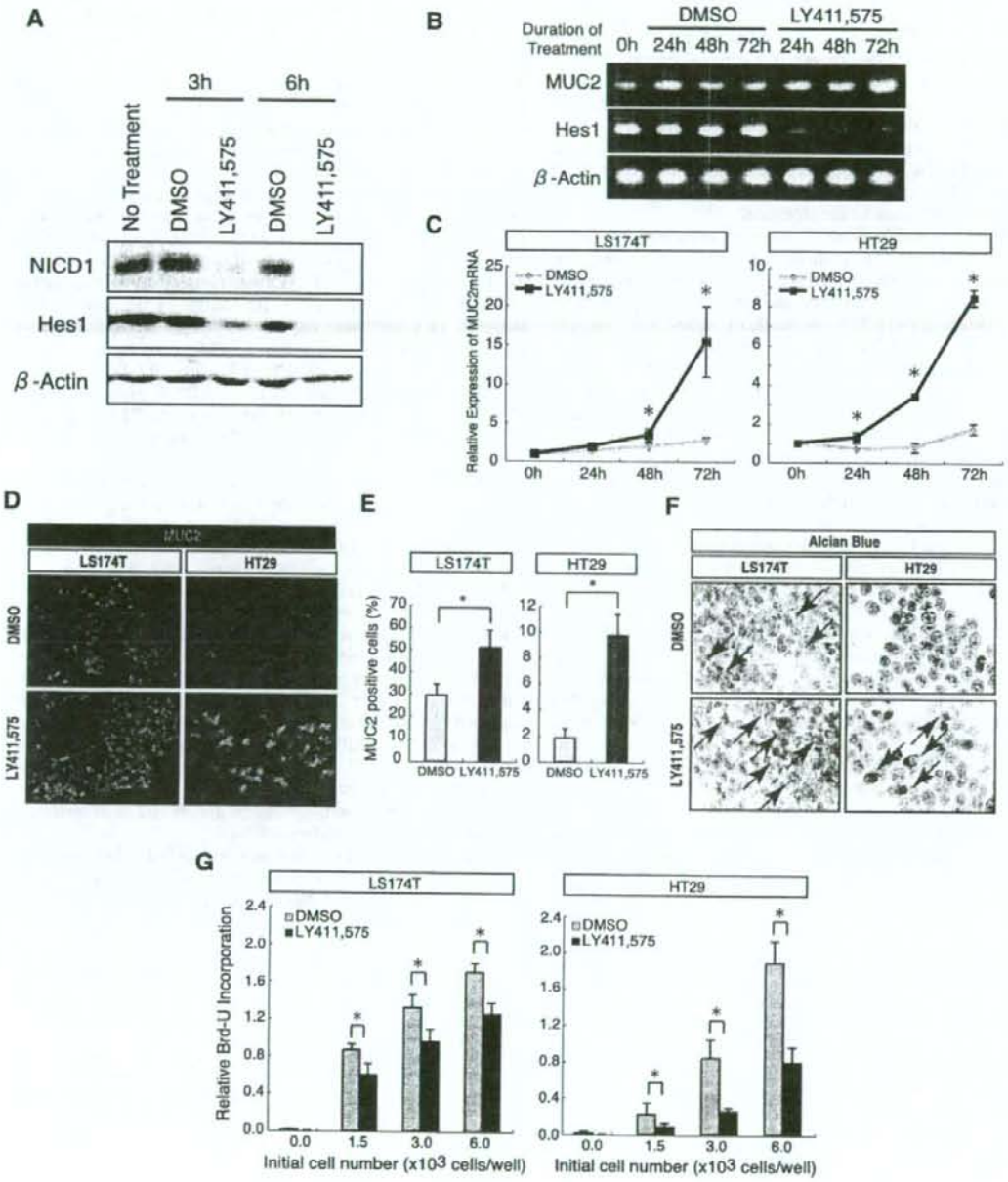

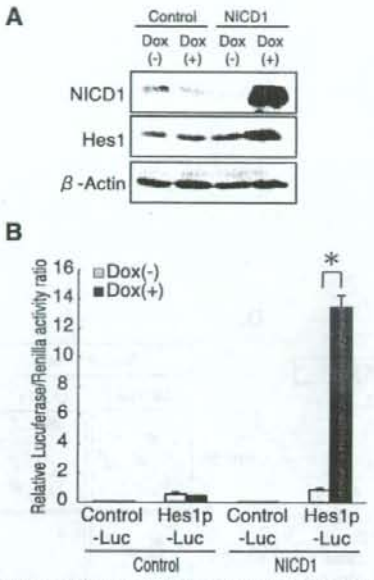

Fig. 4. Activation of Notch1 upregulates Hes1 expression in human IECs. *A*: establishment of a subline of LS174T cells expressing NICD1 under control of a tetracycline-dependent promoter (Tet-On NICD1 cells, designated as NICD1). Immunoblot analysis of Tet-On NICD1 cells showed a clear upregulation of both NICD1 and Hes1 expression with doxycycline (DOX) addition, whereas parental cells (designated as Control) remain unchanged. A low-sensitivity substrate (ECL) was used for visualization. *B*: transcriptional activity of Hes1 was upregulated with the expression of NICD1. Transcriptional activities of Hes1 gene in Tet-On NICD1 cells or control cells were analyzed by luciferase reporter assays using Hes1p-Luc. A reporter plasmid containing only the core-promoter of chicken β-actin gene served as a control (Control-Luc). Luciferase activities were measured after 12 h of culture with or without DOX. Error bars represent SD. $*P < 0.05$ on the Student's *t*-test.

Using this cell line, we found that the upregulation of NICD1 expression in LS174T cells significantly downregulated MUC2 mRNA expression (Fig. 5*A*). Further analysis with a microarray identified a group of genes that were up- or downregulated with NICD1 expression (Supplemental Tables 1 and 2). Among these genes, we focused on PLA2G2A, a gene expressed by Paneth cells, as it showed the most significant induction with NICD1 expression. Quantitative RT-PCR confirmed an upregulation of PLA2G2A mRNA expression with the NICD1 expression (Fig. 5*A*). Consistent with this, although the MUC2 protein expression was markedly suppressed (Fig. 5*B*), with resulting significant decreases in MUC2-positive cells (Fig. 5*C*) and mucin-producing cells (Fig. 5*D*), the PLA2G2A secretion was upregulated with NICD1 expression (Fig. 5*E*). These changes appeared to be regulated at the transcriptional level since the reporter activities of MUC2-Luc and PLA2-Luc showed a significant decrease and increase, respectively, with NICD1 expression (Fig. 5*F*). These results showed that, although the activation of Notch1 within LS174T cells suppressed goblet cell phenotype, it also upregulated the secretion of PLA2G2A, suggesting that the activation of Notch1 might surprisingly promote the acquisition of the specific functions of Paneth cells.

Notch1 is activated in crypt epithelial cells of the human intestine. Since we found that Notch signaling might regulate cell proliferation, goblet cell differentiation, and Paneth cell-specific function within IECs, we sought to clarify its relevance in human intestinal diseases. We first examined whether components of the Notch signaling pathway are expressed in the human intestine. An RT-PCR analysis of human intestinal tissues or epithelial cell lines successfully detected mRNAs of both Notch1 and Hes1 (Fig. 6*A*). The immunohistochemistry for NICD1 and Hes1 revealed that these proteins are expressed in the nuclei of crypt IECs (Fig. 6*B*). Similar to our observations in mice, the distribution of NICD1-positive or Hes1-positive IECs corresponded to that of Ki-67-positive IECs (Fig. 6*B*). Also, a magnified view of the staining showed a positive staining of NICD1 in columnar-shaped IECs and Paneth cells (Fig. 6*B*, black arrow) but not in goblet-shaped IECs (Fig. 6*B*, red arrowhead). Double staining of MUC2 and NICD1 confirmed the lack of NICD1 expression in goblet cells (Fig. 7*A*), whereas double staining of PLA2G2A and NICD1 confirmed expression of NICD1 in Paneth cells (Fig. 7B). These results strongly suggested that the NICD1 might function in vivo in the human intestine in a similar manner as was revealed in the in vitro study.

Increased activation of Notch1 is observed in the mucosa of UC. UC is one of the major forms of inflammatory bowel diseases, characterized by the persistent inflammation and ulcer formation in the colon. In the active region of UC, a loss of goblet cells, an ectopic expression of Paneth cell genes, and an increase in IEC proliferation are all known to be common pathological findings (7, 8, 13, 23). Thus our results strongly suggested that all of these pathological findings in UC might be mediated by the activation of Notch1 in IECs. We performed

Fig. 3. Inhibition of Notch activation promotes differentiation of goblet cells but suppresses proliferation of human IECs. *A*: LY411,575 downregulated expression of Notch1 intracellular domain (NICD1) and Hes1 in LS174T cells. Immunoblot analysis of LS174T cells treated with LY411,575 showing downregulation of endogenous NICD1 and Hes1 expression within 6 h from treatment. Cells treated with DMSO alone served as control. A high-sensitivity substrate (ECL Advance) was used for visualization. *B*: LY411,575 upregulated expression of MUC2 in LS174T cells. LS174T cells were subjected to semiquantitative RT-PCR analysis after treatment with either LY411,575 or DMSO. Note that expression of Hes1 was markedly decreased, whereas expression of MUC2 was increased after 72 h of treatment with LY411,575. *C*: LY411,575 significantly increased expression of MUC2 mRNA in both LS174T and HT29 cells. Cells were subjected to quantitative RT-PCR analysis after 0, 24, 48, and 72 h of treatment with either LY411,575 or DMSO. Error bars represent SD. $*P < 0.05$ for the difference between DMSO and LY411,575 treatment at the same time points on the Student's *t*-test. *D*: LY411,575 induced expression of MUC2 protein (red) in LS174T and HT29 cells. Cells were subjected to immunofluorescent staining of MUC2 after 72 h of treatment with either LY411,575 or DMSO (original magnification ×200). *E*: LY411,575 significantly increased the MUC2-positive cell populations among LS174T and HT29 cells. Quantitative analysis of *D* is shown by percent of MUC2-positive cells within total nucleated cells. Error bars represent SD. $*P < 0.05$, on the Student's *t*-test. *F*: LY411,575 induced mucin production in LS174T and HT29 cells. Cells were subjected to Alcian blue staining (black arrow) after 72 h of treatment with either LY411,575 or DMSO (original magnification ×400). *G*: LY411,575 significantly downregulated proliferation of LS174T and HT29 cells. A significant decrease in BrdU incorporation was observed with LY411,575 treatment in LS174T and HT29 cells. Incorporation of BrdU was measured by ELISA. Results are shown as arbitrary units of relative BrdU incorporation. Error bars represent SD. $*P < 0.05$ on the Student's *t*-test.

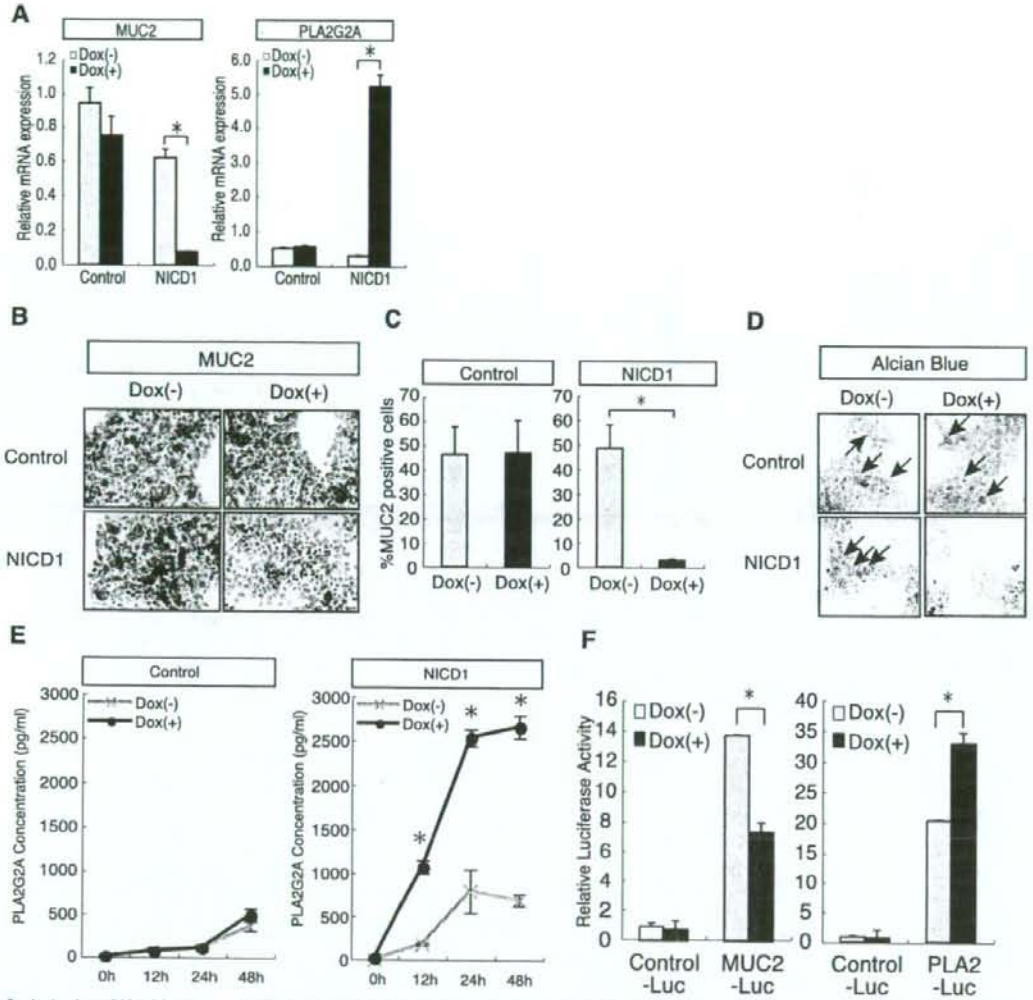

Fig. 5. Activation of Notch1 suppresses goblet cell differentiation but promotes expression of PLA2G2A of human IECs. *A*: expression of NICD1 in LS174T cells downregulated the expression of MUC2 but upregulated the expression of PLA2G2A. Quantitative RT-PCR analysis of MUC2 and PLA2G2A expression in Tet-On NICD1 cells and control cells is shown. Cells were subjected to analysis after 48 h of culture with or without DOX. Error bars represent SD. $*P < 0.05$ on the Student's *t*-test. *B*: expression of NICD1 in LS174T cells downregulated MUC2 protein expression. Tet-On NICD1 cells or control cells were subjected to immunostaining of MUC2 after 48 h of culture with or without DOX. Brown staining with DAB showed positive staining for MUC2 (original magnification ×200). *C*: expression of NICD1 in LS174T cells significantly reduced the number of cells expressing MUC2. Quantitative analysis of immunostaining shown in *B* is shown. Number of cells positively stained for MUC2 was counted and shown as percent of total nucleated cells. Error bars represent SD. $*P < 0.05$ on the Student's *t*-test. *D*: expression of NICD1 suppressed mucin production by LS174T cells. Tet-On NICD1 cells or control cells were treated as described in *B* and subjected to Alcian blue staining. The blue staining represents mucin-producing cells. (black arrow, original magnification ×800). *E*: expression of NICD1 upregulated PLA2G2A secretion of LS174T cells. Tet-On NICD1 cells or control cells were cultured with or without DOX, and culture supernatants collected at various time points were subjected to quantification of PLA2G2A using ELISA. Error bars represent SD. $*P < 0.05$ compared between DOX (+) and DOX (-) on the Student's *t*-test. *F*: expression of NICD1 in LS174T cells downregulated transcriptional activity of MUC2 gene but upregulated transcriptional activity of PLA2G2A gene. Transcriptional activity of MUC2 gene and PLA2G2A gene were measured by luciferase reporter assays using MUC2-Luc and PLA2-Luc as a reporter plasmid, respectively. pGL3-basic served as a control (Control-Luc). Luciferase activities in Tet-On NICD1 cells were analyzed after 12 h of culture with or without DOX. Error bars represent SD. $*P < 0.05$ on the Student's *t*-test.

histological analysis and found that in the crypts of UC, mucin production is markedly decreased (Fig. 8*A*, *top*, blue), whereas the number of Ki-67-expressing cells are markedly increased, distributing from the bottom to the uppermost part of the crypt (Fig. 8*A*, *bottom*, brown). In such crypts, NICD1-expressing cells showed the same distribution as Ki-67-expressing cells (Fig. 8*A*, *middle*, brown), suggesting that Notch1 is activated in an expanded proliferating cell population within the crypts of

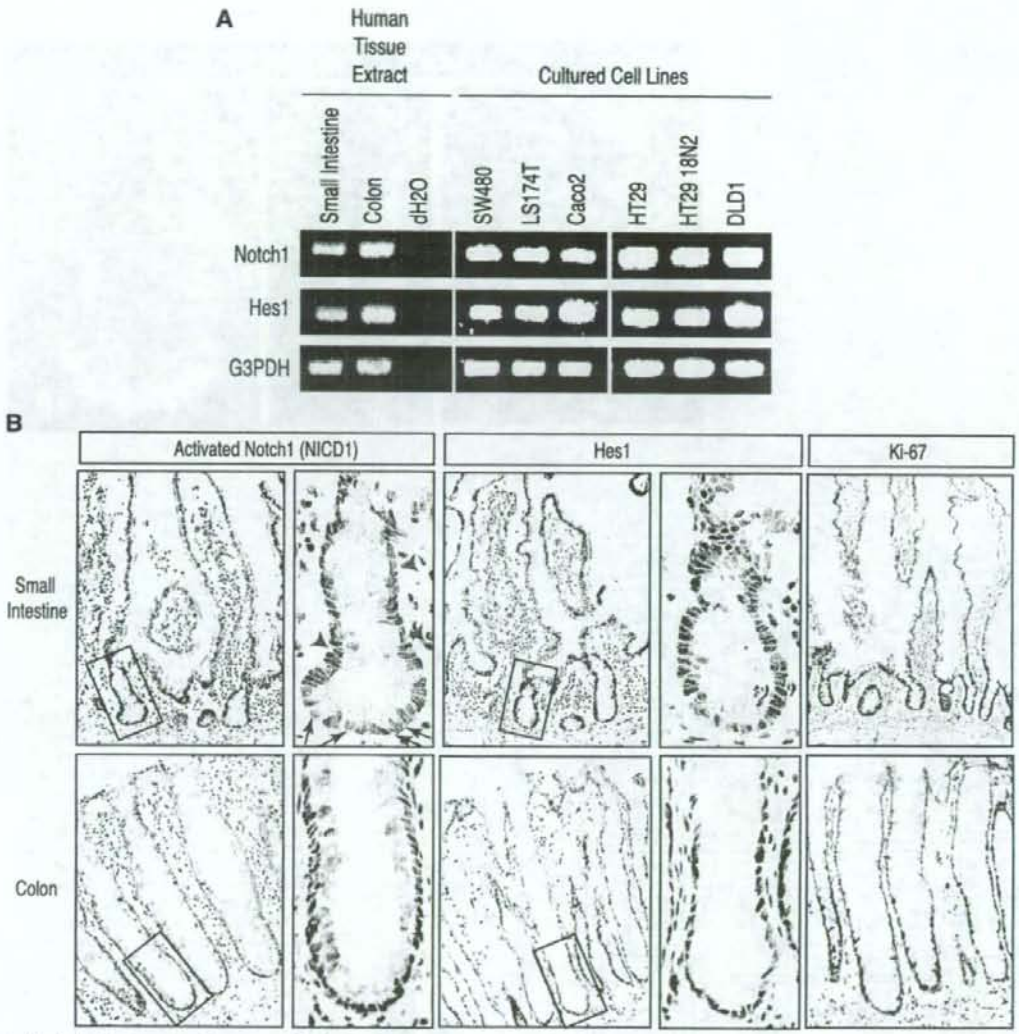

Fig. 6. Notch signaling is activated in crypt epithelial cells of the human intestine. *A*: RT-PCR analysis of human intestinal tissues and human intestinal epithelial cell lines. Expression of both Notch1 and Hes1 are clearly detected in all the examined tissues and cell lines. *B*: immunostaining of human intestinal tissues showing expression of NICD1, Hes1, and Ki-67. Brown staining with DAB showed positive results for NICD1, Hes1, and Ki-67 (original magnification ×200). Magnified view of the squared area is shown in the right side of the original picture (original magnification ×1000). Black arrows show Paneth cells clearly containing granules in the cytoplasm showing positive staining for NICD1, whereas red arrowheads show goblet-shaped cells lacking NICD1 staining.

UC. A quantitative analysis revealed that the number of IECs expressing NICD1 or Ki-67 per crypt is significantly increased, whereas the number of IECs producing mucin is significantly decreased in the crypts of UC (Fig. 8*B*).

We also looked for IECs expressing PLA2G2A within the colonic crypts. There was no expression of PLA2G2A in the crypts of the normal colon (Fig. 9*A*). However, an ectopic expression of PLA2G2A was clearly found in the crypts of the colon epithelia with UC (Fig. 9*B*). Our histological analysis revealed that Notch1 is clearly activated in such IECs ectopically expressing PLA2G2A (Fig. 9, *C* and *D*). Such activation of Notch1 in PLA2G2A-expressing cells could also be found in less inflamed regions of UC where there were fewer PLA2G2A-expressing IECs (Fig. 9, *E* and *F*).

From these results, we confirmed that Notch1 is activated in a greater number of crypt IECs in UC, presumably mediating goblet cell depletion, cell proliferation, and ectopic expression of PLA2G2A. We suggest that such Notch1-mediated changes

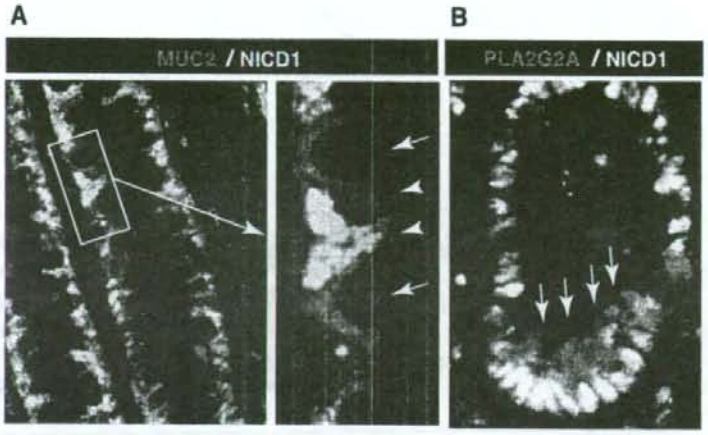

Fig. 7. Human Notch1 is not activated in IECs expressing MUC2 but is activated in IECs expressing PLA2G2A. *A*: human Notch1 was not activated in IECs expressing MUC2 in vivo. Double staining for MUC2 (red) and NICD1 (green) using human colonic tissue is shown. NICD1 and MUC2 were expressed in distinct populations of epithelial cells (*left*, ×400). A magnified view (*right*, ×1600) clearly shows cytoplasmic staining of MUC2 in goblet-shaped cells (yellow arrow), whereas nuclear staining of NICD1 in columnar-shaped cells (white arrowhead). *B*: human Notch1 is activated in IECs expressing PLA2G2A in vivo. Double staining for PLA2G2A (red) and NICD1 (green) using a human small intestinal tissue is shown. NICD1 and PLA2G2A were coexpressed in IECs residing at the lowest part of the crypt, suggesting activation of Notch1 in Paneth cells (yellow arrow, original magnification ×1000).

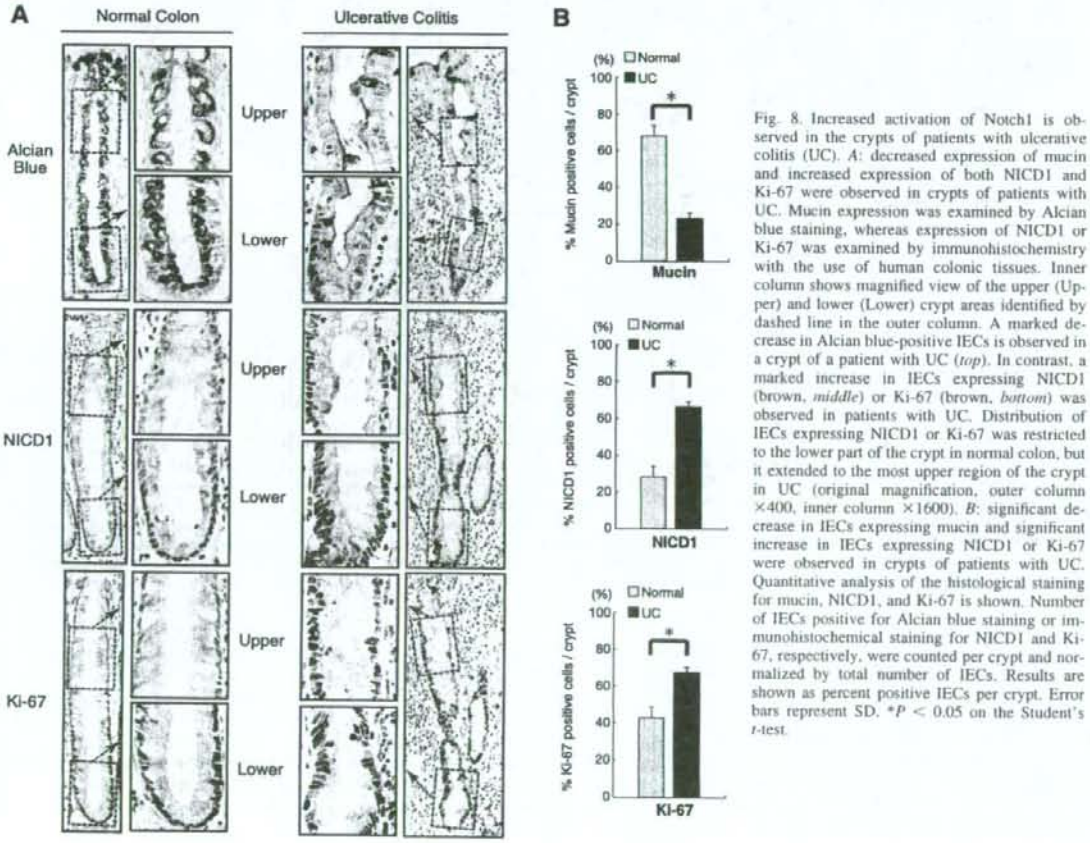

Fig. 8. Increased activation of Notch1 is observed in the crypts of patients with ulcerative colitis (UC). *A*: decreased expression of mucin and increased expression of both NICD1 and Ki-67 were observed in crypts of patients with UC. Mucin expression was examined by Alcian blue staining, whereas expression of NICD1 or Ki-67 was examined by immunohistochemistry with the use of human colonic tissues. Inner column shows magnified view of the upper (Upper) and lower (Lower) crypt areas identified by dashed line in the outer column. A marked decrease in Alcian blue-positive IECs is observed in a crypt of a patient with UC (*top*). In contrast, a marked increase in IECs expressing NICD1 (brown, *middle*) or Ki-67 (brown, *bottom*) was observed in patients with UC. Distribution of IECs expressing NICD1 or Ki-67 was restricted to the lower part of the crypt in normal colon, but it extended to the most upper region of the crypt in UC (original magnification, outer column ×400, inner column ×1600). *B*: significant decrease in IECs expressing mucin and significant increase in IECs expressing NICD1 or Ki-67 were observed in crypts of patients with UC. Quantitative analysis of the histological staining for mucin, NICD1, and Ki-67 is shown. Number of IECs positive for Alcian blue staining or immunohistochemical staining for NICD1 and Ki-67, respectively, were counted per crypt and normalized by total number of IECs. Results are shown as percent positive IECs per crypt. Error bars represent SD. $^*P < 0.05$ on the Student's *t*-test.

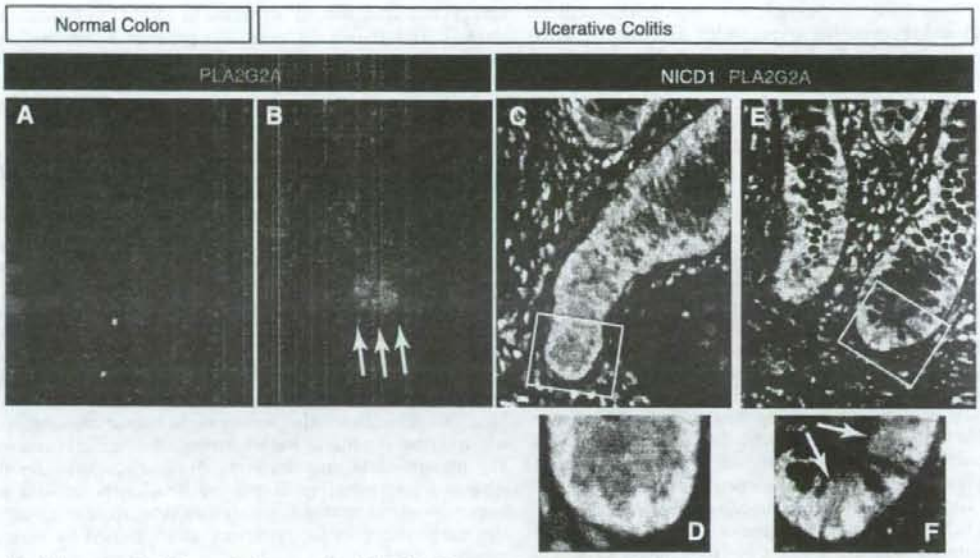

Fig. 9. Notch1 is activated in IECs ectopically expressing PLA2G2A. Fluorescent immunostaining for PLA2G2A (red) was completely negative in the crypts of normal colon (*A*, original magnification ×400), whereas some of the IECs in the crypts of a patient with UC were clearly positive for PLA2G2A (*B*, yellow arrow, original magnification ×400). Some cells in the lamina propria were also positive for PLA2G2A. Double immunostaining for NICD1 (green) and PLA2G2A (red) showed coexpression of NICD1 and PLA2G2A by colonic IECs of a patient with UC (*C–F*). In the inflamed region (*C, D*), NICD1 was expressed in most parts of the crypt IECs, and some proportion of those IECs coexpressed PLA2G2A (*C*, original magnification ×400). A magnified view (*D*, original magnification ×1000) of the indicated region (white square in *C*) clearly showed a nuclear distribution of NICD1 and a cytoplasmic distribution of PLA2G2A. In a less inflamed region, few IECs appeared to be positive for both NICD1 and PLA2G2A (*E*, original magnification ×400). Magnified view of the indicated region (white square in *E*) confirms coexpression of NICD1 and PLA2G2A in the nucleus and cytoplasm of an IEC, respectively (*F*, yellow arrow, original magnification ×1000).

observed in the mucosa of UC are not detrimental changes contributing to the persistence of the disease, but rather they are positive responses that help to regenerate the damaged epithelia, thereby aggressively contributing to the termination and recovery from the disease.

DISCUSSION

To date, several studies using knockout mice have revealed various functions of Notch signaling in IECs; one critical function is that of regulating the cell fates of IECs (31). The recent model accepted in such studies implicates Notch activation as a positive regulator of absorptive cell differentiation but a negative regulator of the differentiation of secretory lineage cells, including goblet cells. However, studies have suggested that Notch activation not only acts to determine the cell fates of progenitor IECs, but it may also regulate the number of proliferating populations within the crypt (6, 28, 33). Our results are consistent with the previous observations, and they further highlight the critical role of Notch activation in a situation when the rapid expansion of IECs is required (e.g., during the regeneration process in UC). Since the in vivo phenotype of Notch inhibition showed not only the loss of absorptive lineage cells but also the loss of the entire epithelial layer, this suggested that the activation of Notch may contribute to the expansion of both absorptive and secretory precursor cells and even stem cells. This is consistent with the observation by Vooijs et al. (34) that IECs that matured into absorptive cells must have also experienced Notch activation during development from the stem cell. Thus our results demonstrated the importance of Notch activation in the expansion of multilineage precursor IECs, whose function becomes critically required when tissue damage is present. In contrast, although Notch activation was predominant in the proliferating IECs of the colitic mucosa, its role in postmitotic IECs might be of less importance (42).

A recent study has shown that the chronic inhibition of Notch activation using LY411,575 (for up to 15 consecutive days) could impair the development of lymphoid cells (14, 36). Thus it may be possible that such an effect of LY411,575 might have altered the local immune function of the DSS-treated mice and thereby exacerbated their colitis. Indeed, LY411,575 proved to have a systemic effect, especially on the development of thymocytes (Supplemental Fig. S1). However, no effect was observed on splenocytes (Supplemental Fig. S1). Also, no effect was observed on local production of proinflammatory cytokines (Supplemental Fig. S2). Thus, although it is possible that LY411,575 might have some effect on the inflammatory response, its involvement on the exacerbation of the present colitis model may be minimal.

Also, GSI has been reported to promote the differentiation and inhibit proliferation of mice intestinal adenoma through the inhibition of Notch activation (33). Therefore, GSIs have been reported to have an antitumor effect (32). However, our results showed that the effects of GSIs may not be specific for tumor

cells. GSIs have almost the same effect on progenitor cells of the normal and regenerating crypt, which becomes critically toxic once the epithelia have been damaged. Thus caution is needed with the use of GSIs when intestinal tissue damage is present.

Although studies have revealed various extrinsic factors promoting the regeneration of the intestinal epithelia (2, 3), the intracellular mechanism mediating the regenerative process has not been fully elucidated (15). Our data show that Notch activation maintains the larger number of IECs in the immature state, thereby promoting the proliferation and supporting the rapid recovery of IECs needed to restore proper epithelial structure. Thus we identified Notch signaling as one of the main intracellular pathways mediating the organized regenerative response of the intestinal epithelia. Although we know that several ligands and receptors of the Notch pathway are expressed in the intestine (24, 26), we do not know the precise mechanism by which these ligands activate Notch receptors, in particular IECs. A recent study by Riccio et al. (22) clearly showed that both Notch1 and Notch2 function redundantly in the intestinal epithelia and that they directly regulate the cell cycle progression of crypt progenitor cells. Thus an analysis of the Notch ligand expression is needed to understand the mechanism by which these Notch receptors could be activated during epithelial regeneration and the mechanism by which such activation could be downregulated at the later stage of regeneration.

One of our surprising findings was the upregulation of PLA2G2A in Notch-activated IECs, suggesting that Notch might also modulate immune functions of IECs. PLA2G2A is usually expressed in Paneth cells, and it is known to have an antimicrobial effect (4). The loss of the continuity of the epithelial layer allows various and abundant microorganisms to invade the submucosal area, thereby promoting inflammation and further destruction of the mucosa. Thus the local secretion of PLA2G2A at the damaged mucosal area may be quite beneficial for limiting bacterial invasion and providing a proper environment for regeneration. However, previous reports have shown that PLA2G2A is also expressed by neutrophils and macrophages accumulating at the inflamed mucosa of colitis (29, 39). Consistent with this, we observed an infiltration of PLA2G2A-positive cells in the lamina propria of inflamed mucosa in UC (Fig. 9, *C–F*). An RT-PCR analysis of DSS-colitis showed a significant upregulation of PLA2G2A expression in the inflamed colonic mucosa (Supplemental Fig. S3). However, such an upregulation was not inhibited with LY411,575 treatment, suggesting that the expression of PLA2G2A by neutrophils or macrophages might be less dependent on Notch activation. In those cells, intracellular pathways such as NF-κB might function to promote expression of PLA2G2A in the inflamed colonic mucosa (37). Also, our histological analysis suggested that the upregulation of PLA2G2A secretion was not a general but a partial response in Notch-activated IECs, indicating that an additional condition is required for ectopic expression of PLA2G2A.

Our microarray analysis also revealed a number of genes other than PLA2G2A that are regulated by NICD1 in IECs. Although the results did not show an upregulation of other genes specific to Paneth cells such as lysozyme or α-defensins, our quantitative RT-PCR confirmed that genes such as clusterin or spermidine/spermine N1-acetyltransferase were also upregulated upon Notch1 activation in LS174T cells (data not shown). Trefoil factor-1 may also promote Notch-mediated tissue regeneration because it is known to be a key factor in restitution (11). The group of genes shown in the present analysis was quite distinct from the previous microarray analysis comparing GSI-treated and untreated intestinal tissues (14, 27). Because we used an in vitro IEC-based assay, the group of genes identified can be recognized as candidates of the IEC-specific target genes of Notch. However, because only a limited number of genes were analyzed (up to 10,000 annotated genes) in the present study, a further analysis including a larger group of genes may elucidate additional genes that are regulated downstream of Notch.

In conclusion, Notch signaling acts as an indispensable intracellular signaling pathway in IECs, especially during tissue regeneration. It regulates not only the differentiation, but also the proliferation of IECs, and it also regulates the immune function of IECs. We have shown for the first time that such functions of Notch are also present in the human intestine, both under normal conditions and when tissue damage has occurred. The present study provides a novel molecular basis for the advanced understanding of the regeneration process in the human intestinal epithelia, which may be utilized to establish alternative therapies for refractory ulcers caused by various intestinal diseases.

ACKNOWLEDGMENTS

The authors thank Dr. Tetsuo Sudo for providing the Hes1 antibody, Drs. Ryoichiro Kageyama and Yasuhito Yuasa for providing the plasmids, Drs. Hisao Fukushima, Kazutaka Koganei, Kenichi Sugihara, and Hiroyuki Uetake for providing the tissue samples, Drs. Hideyuki Okano and Takaaki Ito for the helpful discussion, and Dr. Hisanobu Kawamura, Dr. Michio Onizawa, and Ms. Motomi Yamazaki for technical assistance.

GRANTS

This study was supported in part by grants-in-aid for Scientific Research, Scientific Research on Priority Areas, Exploratory Research, and Creative Scientific Research from the Japanese Ministry of Education, Culture, Sports, Science and Technology, The Japanese Ministry of Health, Labor and Welfare, The Japanese Society of Gastroenterology, The Foundation for Advancement of International Science, Research Fund of Mitsukoshi Health and Welfare Foundation, and the Research Fund of Japan Intractable Diseases Research Foundation.

REFERENCES

1. **Bjerknes M, Cheng H.** Gastrointestinal stem cells. II. Intestinal stem cells. *Am J Physiol Gastrointest Liver Physiol* 289: G381–G387, 2005.
2. **Bjerknes M, Cheng H.** Modulation of specific intestinal epithelial progenitors by enteric neurons. *Proc Natl Acad Sci USA* 98: 12497–12502, 2001.
3. **Brauchle M, Madlener M, Wagner AD, Angermeyer K, Lauer U, Hofschneider PH, Gregor M, Werner S.** Keratinocyte growth factor is highly overexpressed in inflammatory bowel disease. *Am J Pathol* 149: 521–529, 1996.
4. **Buckland AG, Wilton DC.** The antibacterial properties of secreted phospholipases A(2). *Biochim Biophys Acta* 1488: 71–82, 2000.
5. **Fahlgren A, Hammarstrom S, Danielsson A, Hammarstrom ML.** Increased expression of antimicrobial peptides and lysozyme in colonic epithelial cells of patients with ulcerative colitis. *Clin Exp Immunol* 131: 90–101, 2003.
6. **Fre S, Huyghe M, Mourikis P, Robine S, Louvard D, Artavanis-Tsakonas S.** Notch signals control the fate of immature progenitor cells in the intestine. *Nature* 435: 964–968, 2005.
7. **Haapamaki MM, Gronroos JM, Nurmi H, Alanen K, Kallajoki M, Nevalainen TJ.** Gene expression of group II phospholipase A2 in intestine in ulcerative colitis. *Gut* 40: 95–101, 1997.
8. **Haapamaki MM, Gronroos JM, Nurmi H, Irjala K, Alanen KA, Nevalainen TJ.** Phospholipase A2 in serum and colonic mucosa in ulcerative colitis. *Scand J Clin Lab Invest* 59: 279–287, 1999.

9. **Jensen J, Pedersen EE, Galante P, Hald J, Heller RS, Ishibashi M, Kageyama R, Guillemot F, Serup P, Madsen OD.** Control of endodermal endocrine development by Hes-1. *Nat Genet* 24: 36–44, 2000.
10. **Kopan R.** Notch: a membrane-bound transcription factor. *J Cell Sci* 115: 1095–1097, 2002.
11. **Longman RJ, Douthwaite J, Sylvester PA, Poulsom R, Corfield AP, Thomas MG, Wright NA.** Coordinated localisation of mucins and trefoil peptides in the ulcer associated cell lineage and the gastrointestinal mucosa. *Gut* 47: 792–800, 2000.
12. **Matsumoto T, Okamoto R, Yajima T, Mori T, Okamoto S, Ikeda Y, Mukai M, Yamazaki M, Oshima S, Tsuchiya K, Nakamura T, Kanai T, Okano H, Inazawa J, Hibi T, Watanabe M.** Increase of bone marrow-derived secretory lineage epithelial cells during regeneration in the human intestine. *Gastroenterology* 128: 1851–1867, 2005.
13. **McCormick DA, Horton LW, Mee AS.** Mucin depletion in inflammatory bowel disease. *J Clin Pathol* 43: 143–146, 1990.
14. **Milano J, McKay J, Dagenais C, Foster-Brown L, Pognan F, Gadient R, Jacobs RT, Zacco A, Greenberg B, Ciaccio PJ.** Modulation of notch processing by gamma-secretase inhibitors causes intestinal goblet cell metaplasia and induction of genes known to specify gut secretory lineage differentiation. *Toxicol Sci* 82: 341–358, 2004.
15. **Okamoto R, Watanabe M.** Cellular and molecular mechanisms of the epithelial repair in IBD. *Dig Dis Sci*, 50 *Suppl* 1: S34–S38, 2005.
16. **Okamoto R, Watanabe M.** Molecular and clinical basis for the regeneration of human gastrointestinal epithelia. *J Gastroenterol* 39: 1–6, 2004.
17. **Okayasu I, Hatakeyama S, Yamada M, Ohkusa T, Inagaki Y, Nakaya R.** A novel method in the induction of reliable experimental acute and chronic ulcerative colitis in mice. *Gastroenterology* 98: 694–702, 1990.
18. **Oshima S, Nakamura T, Namiki S, Okada E, Tsuchiya K, Okamoto R, Yamazaki M, Yokota T, Aida M, Yamaguchi Y, Kanai T, Handa H, Watanabe M.** Interferon regulatory factor 1 (IRF-1) and IRF-2 distinctively upregulate gene expression and production of interleukin-7 in human intestinal epithelial cells. *Mol Cell Biol* 24: 6298–6310, 2004.
19. **Podolsky DK.** Healing the epithelium: solving the problem from two sides. *J Gastroenterol* 32: 122–126, 1997.
20. **Radtke F, Clevers H, Riccio O.** From gut homeostasis to cancer. *Curr Mol Med* 6: 275–289, 2006.
21. **Rakoff-Nahoum S, Paglino J, Eslami-Varzaneh F, Edberg S, Medzhitov R.** Recognition of commensal microflora by toll-like receptors is required for intestinal homeostasis. *Cell* 118: 229–241, 2004.
22. **Riccio O, van Gijn ME, Bezdek AC, Pellegrinet L, van Es JH, Zimber-Strobl U, Strobl LJ, Honjo T, Clevers H, Radtke F.** Loss of intestinal crypt progenitor cells owing to inactivation of both Notch1 and Notch2 is accompanied by derepression of CDK inhibitors p27Kip1 and p57Kip2. *EMBO Rep* 9: 377–383, 2008.
23. **Riddle RH.** *Pathology of Idiopathic Inflammatory Bowel Disease*. Orlando, FL: Saunders, 2004.
24. **Sander GR, Powell BC.** Expression of notch receptors and ligands in the adult gut. *J Histochem Cytochem* 52: 509–516, 2004.
25. **Sasai Y, Kageyama R, Tagawa Y, Shigemoto R, Nakanishi S.** Two mammalian helix-loop-helix factors structurally related to Drosophila hairy and Enhancer of split. *Genes Dev* 6: 2620–2634, 1992.
26. **Schroder N, Gossler A.** Expression of Notch pathway components in fetal and adult mouse small intestine. *Gene Expr Patterns* 2: 247–250, 2002.
27. **Searfoss GH, Jordan WH, Calligaro DO, Galbreath EJ, Schirtzinger LM, Berridge BR, Gao H, Higgins MA, May PC, Ryan TP.** Adipsin, a biomarker of gastrointestinal toxicity mediated by a functional gamma-secretase inhibitor. *J Biol Chem* 278: 46107–46116, 2003.
28. **Stanger BZ, Datar R, Murtaugh LC, Melton DA.** Direct regulation of intestinal fate by Notch. *Proc Natl Acad Sci USA* 102: 12443–12448, 2005.
29. **Tomita Y, Jyoyama H, Kobayashi M, Kuwahara K, Furue S, Ueno M, Yamada K, Ono T, Teshirogi I, Nomura K, Arita H, Okayasu I, Hori Y.** Role of group IIA phospholipase A2 in rat colitis induced by dextran sulfate sodium. *Eur J Pharmacol* 472: 147–158, 2003.
30. **Tsuchiya K, Nakamura T, Okamoto R, Kanai T, Watanabe M.** Reciprocal targeting of Hath1 and beta-catenin by Wnt glycogen synthase kinase 3beta in human colon cancer. *Gastroenterology* 132: 208–220, 2007.
31. **van Den Brink GR, de Santa Barbara P, Roberts Development DJ.** Epithelial cell differentiation—a Mather of choice. *Science* 294: 2115–2116, 2001.
32. **van Es JH, Clevers H.** Notch and Wnt inhibitors as potential new drugs for intestinal neoplastic disease. *Trends Mol Med* 11: 496–502, 2005.
33. **van Es JH, van Gijn ME, Riccio O, van den Born M, Vooijs M, Begthel H, Cozijnsen M, Robine S, Winton DJ, Radtke F, Clevers H.** Notch/gamma-secretase inhibition turns proliferative cells in intestinal crypts and adenomas into goblet cells. *Nature* 435: 959–963, 2005.
34. **Vooijs M, Ong CT, Hadland B, Huppert S, Liu Z, Korving J, van den Born M, Stappenbeck T, Wu Y, Clevers H, Kopan R.** Mapping the consequence of Notch1 proteolysis in vivo with NIP-CRE. *Development* 134: 535–544, 2007.
35. **Watanabe M, Ueno Y, Yajima T, Okamoto S, Hayashi T, Yamazaki M, Iwao Y, Ishii H, Habu S, Uehira M, Nishimoto H, Ishikawa H, Hata J, Hibi T.** Interleukin 7 transgenic mice develop chronic colitis with decreased interleukin 7 protein accumulation in the colonic mucosa. *J Exp Med* 187: 389–402, 1998.
36. **Wong GT, Manfra D, Poulet FM, Zhang Q, Josien H, Bara T, Engstrom L, Pinzon-Ortiz M, Fine JS, Lee HJ, Zhang L, Higgins GA, Parker EM.** Chronic treatment with the gamma-secretase inhibitor LY-411,575 inhibits beta-amyloid peptide production and alters lymphopoiesis and intestinal cell differentiation. *J Biol Chem* 279: 12876–12882, 2004.
37. **Wu F, Chakravarti S.** Differential expression of inflammatory and fibrogenic genes and their regulation by NF-kappaB inhibition in a mouse model of chronic colitis. *J Immunol* 179: 6988–7000, 2007.
38. **Wu J, Tung JS, Thorsett ED, Pleiss MA, Nissen JS, Neitz J, Latimer JH, John V, Freedman S,** inventors. Cycloalkyl, Lactam, Lactone and related compounds as β-amyloid peptide release inhibitors. US patent WO-1998028268, February 7, 1998.
39. **Yamaguchi O, Sugimura K, Ishizuka K, Suzuki K, Hasegawa K, Ohtsuka K, Honma T, Asakura H.** Correlation between serum phospholipase A(2) IIA levels and histological activity in patients with ulcerative colitis. *Int J Colorectal Dis* 17: 311–316, 2002.
40. **Yamamoto H, Bai YQ, Yuasa Y.** Homeodomain protein CDX2 regulates goblet-specific MUC2 gene expression. *Biochem Biophys Res Commun* 300: 813–818, 2003.
41. **Yamazaki M, Yajima T, Tanabe M, Fukui K, Okada E, Okamoto R, Oshima S, Nakamura T, Kanai T, Uehira M, Takeuchi T, Ishikawa H, Hibi T, Watanabe M.** Mucosal T cells expressing high levels of IL-7 receptor are potential targets for treatment of chronic colitis. *J Immunol* 171: 1556–1563, 2003.
42. **Zecchini V, Domaschenz R, Winton D, Jones P.** Notch signaling regulates the differentiation of post-mitotic intestinal epithelial cells. *Genes Dev* 19: 1686–1691, 2005.

症 例

パルミチン酸デキサメタゾンの静注が有効であった単純性潰瘍の1例

島谷昌明　松下光伸　若松隆宏　大宮美香　内田一茂
高岡　亮　關　壽人　岡崎和一

関西医科大学 第3内科

要　旨

症例は40歳女性．咽頭潰瘍にて当院耳鼻科に入院．プレドニゾロン静注にて咽頭潰瘍は軽快したが，下腹部痛を認めた．大腸内視鏡で，回腸末端部に下掘れ潰瘍があり，単純性潰瘍と診断した．経口ステロイドを開始したが，効果に乏しく，パルミチン酸デキサメタゾンの静注を行い瘢痕化した．難治性単純性潰瘍に対するパルミチン酸デキサメタゾンの効果を内視鏡的に観察し得た症例を経験したので報告する．

Key words　単純性潰瘍／リポ化ステロイド／パルミチン酸デキサメタゾン

I　緒　言

単純性潰瘍は主として回盲部に発生する難治性・易再発性で原因不明の慢性炎症性腸疾患である．肉眼的には境界明瞭な円形ないし卵円形の打ち抜き様の深い潰瘍を特徴とし，組織学的には慢性活動性の非特異性炎症像を示す[1),2)]．単純性潰瘍は回盲弁上ないしその近傍に好発し，腸管ベーチェット病の潰瘍と肉眼的にも病理組織学的にも鑑別は困難である[3)~5)]．また，本疾患の発生頻度も高くないため，まとまった報告も少なく，治療法も十分には確立されていないのが現状であるが[5)~9)]，内科的治療が奏功する例と，穿孔・出血を繰り返す難治例が認められる．今回，パルミチン酸デキサメタゾン（リポ化ステロイド）の静注が回腸末端部病変に有効であった単純性潰瘍の1例を経験し，その効果を内視鏡的に観察し得たので報告する．

Gastroenterol Endosc 2008；50：1109-14.
Masaaki SHIMATANI
Effective Palmit-Dexamethasone Incorporated in Lipid Emulsion for Refractory Simple Ulcer.

別刷請求先：〒573-1191 大阪府枚方市新町2丁目3-1
関西医科大学 第3内科　島谷昌明

II　症　例

症例：40歳，女性．

主訴：咽頭痛，下腹部痛．

家族歴：特記すべきことなし．

既往歴：特記すべきことなし．

現病歴：平成17年2月4日より咽頭痛にて近医受診し咽頭潰瘍を認め，経口ステロイド剤の投与を受けたが胃部不快感，肝機能障害を認めたうえ自覚症状の改善も認められなかった．2月末よ

Table 1　入院時検査成績．

CBC		**Biochemistry**	
WBC	11,200 /μl	TP	6.7 g/dl
RBC	440×10⁴/μl	ALB	3.7 g/dl
Hb	11.2 g/dl	BS	115 mg/dl
Ht	36.3 %	Na	141 mEq/l
PLT	44.5×10⁴/μl	K	3.8 mEq/l
		BUN	8 mg/dl
Serological Tests		Cr	0.5 mg/dl
ANA	20以下 倍	AST	18 U/l
RA	5 IU/ml	ALT	12 U/l
CH50	58.4 単位	T-Bil	0.2 mg/dl
C3	138 mg/dl	ALP	386 U/l
C4	30 mg/dl	LDH	160 U/l
ESR	71 mm/h		
CRP	3.5 mg/dl	**Tumor Markers**	
		CEA	2.9 ng/ml
Culture of ileal mucosa		CA19-9	8.5 U/ml
M. tuberculosis negative			

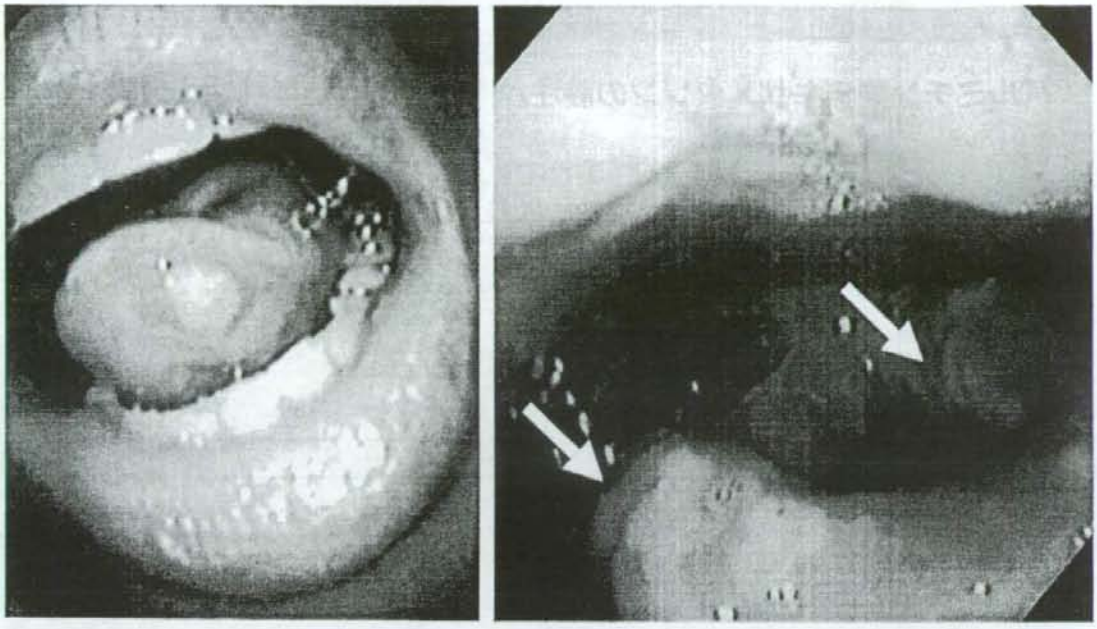

a　　b

Figure 1　咽喉頭鏡検査．
a：口腔内アフタを認めた．
b：咽喉頭に白苔を伴う潰瘍性病変を認めた．

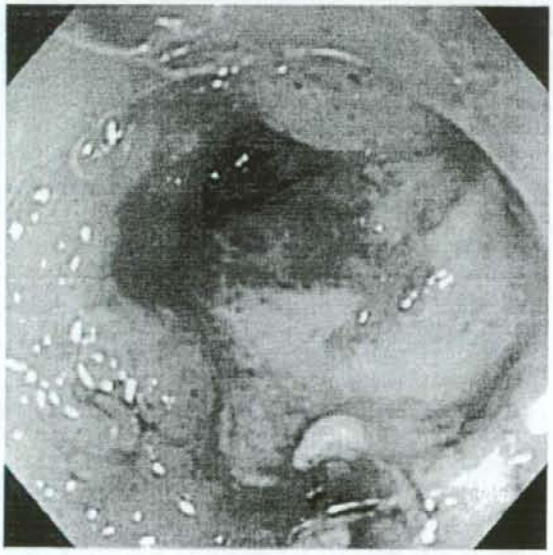

Figure 2　大腸内視鏡検査（初回）．
回盲弁の発赤，回腸末端部に下掘れ傾向の強い潰瘍を認め，周囲粘膜は発赤・浮腫が強く，やや狭窄も伴っていた．

り発熱も認め，経口摂取も困難になったため3月中旬に当院耳鼻科に紹介入院となった．プレドニゾロン静注（100 mg/日，60 mg/日，40 mg/日，20 mg/日各2日間，計8日間投与）にて咽頭潰瘍は軽快したが，以前より下痢と便秘を繰り返し下腹部痛も認めるため精査目的にて当科紹介受診となった．

初診時現症：身長140 cm，体重39 kg，体温36.9℃，血圧100/72 mmHg，心拍数60/分・整，呼吸数20/分，全身状態良好，意識清明，結膜に貧血・黄疸認めず，表在リンパ節触知せず．口腔内アフタを数個認める．胸部聴診上異常なし．腹部平坦，軟，右下腹部に圧痛を認める．外陰部潰瘍および眼病変は認めなかった．神経学的にも異常所見を認めなかった．

検査成績（Table 1）：軽度の貧血と白血球数増加を認め，赤沈値71.0 mm/時と亢進，CRP 3.5 mg/dlと上昇を認めた．また，肝機能異常も認めた．補体価58.4単位，C4 138 mg/dlと軽度上昇を認めるが，各種自己抗体は陰性であった．

咽喉頭鏡検査（Figure 1）：咽喉頭に白苔を伴う潰瘍性病変を認めた．

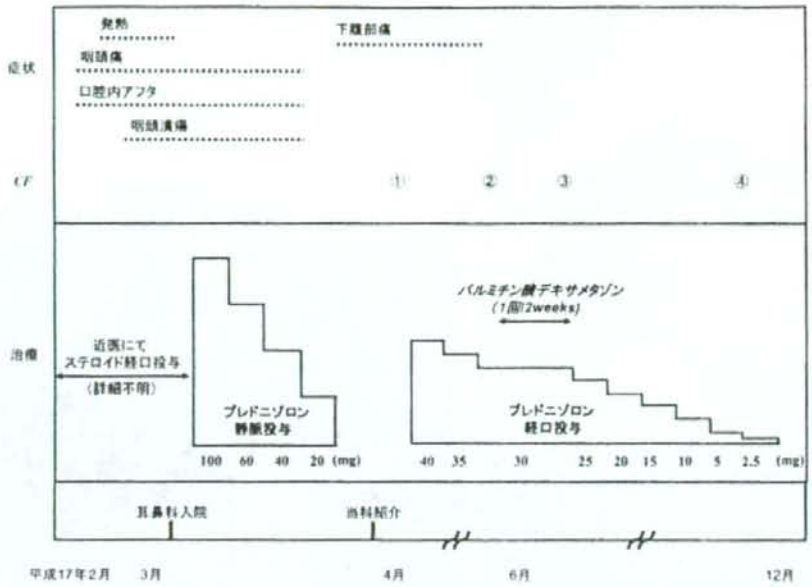

Figure 3　臨床経過.

大腸内視鏡検査（初回）(Figure 2)：回盲弁の発赤，回腸末端部に下掘れ傾向の強い潰瘍を認めた．その周囲粘膜は発赤・浮腫が強く，やや狭窄も伴い，これより口側へは挿入しなかった．

生検病理所見：H&E 染色では，非特異的炎症所見のみで，特異的な肉芽腫は認めなかった．

経過(Figure 3)：口腔内アフタは認めるが，陰部潰瘍，眼症状，皮膚症状を伴わず腸管ベーチェット病の診断基準は満たさなかった．また，クローン病，潰瘍性大腸炎，腸結核などに見られるような組織所見も得られないことから単純性潰瘍と診断し，4月末より経口プレドニゾロン 40 mg を開始した．腹部症状は軽快傾向にあり徐々に 30 mg までプレドニゾロンを減量したが，6月初旬(経口プレドニゾロン開始6週後)の2回目の大腸内視鏡では，回腸末端部の潰瘍周囲の浮腫・狭窄は改善傾向にあったが，依然下掘れ傾向の強い潰瘍が認められた(Figure 4)．そこで，十分なインフォームドコンセント後に6月中旬よりパルミチン酸デキサメタゾン（リポ化ステロイド）4.0 mg の静注を2週間ごとに計6回行った．その間，経口プレドニゾロン 30 mg は持続投与していた．パルミチン酸デキサメタゾン投与終了後，9月初旬の3回目の大腸内視鏡では，回腸末端部の潰瘍は，肉牛上皮が出現し瘢痕化が認められ著明に改善していた(Figure 5)．9月初旬より経口プレドニゾロン 25 mg に減量し，以後2週間ごとに減量を行ったが，腹部症状の増悪は認めなかった．12月初旬の4回目の大腸内視鏡検査では，回腸末端部の潰瘍はほぼ治癒していた(Figure 6)．経口プレドニゾロンを漸減した後中止したが，自覚症状の悪化を認めず経過観察中で，平成 18 年9月の大腸内視鏡検査では，回腸末端部潰瘍の再発も認めていない．

III　考　按

単純性潰瘍は腸管ベーチェット病の腸潰瘍と肉眼的病理組織学的には全く同一の，比較的境界明瞭な下掘れ傾向の強い潰瘍を，主として回盲弁上およびその近傍に生じる再発性・難治性疾患である[1-5]．単純性潰瘍に比較的よく合併する症状として，再発性・難治性の口腔粘膜アフタがあげられるが，再発性・難治性の口腔粘膜アフタの症例の中で単純性潰瘍の併存がどの程度の頻度を占めるかは未だ不明である．単純性潰瘍に口腔内アフタを合併する症例は報告されているが，深い咽頭潰瘍を合併した症例は報告が少なく，文献的には深い咽頭潰瘍と単純性潰瘍の予後との関連性は明らかでない．単なる再発性の口腔粘膜アフタのみでなく咽頭潰瘍まできたす症例では腸潰瘍の出

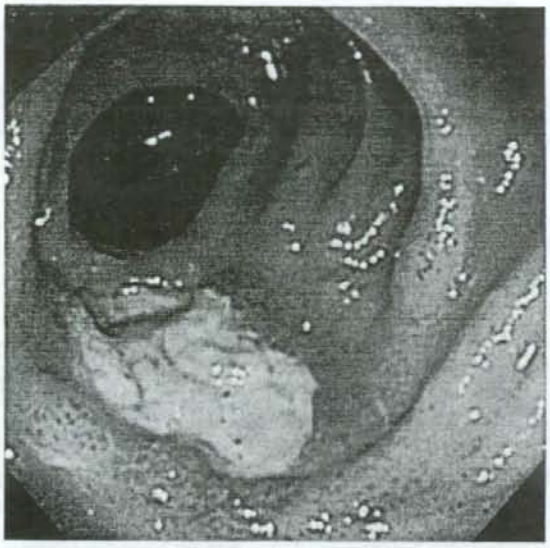

Figure 4　大腸内視鏡検査（2回目）.
経口プレドニゾロン開始6週後.
潰瘍周囲の浮腫・狭窄は改善傾向にあるも，下掘れ傾向の強い潰瘍は依然認められた．また，口側小腸にも潰瘍性病変は数カ所認められた.

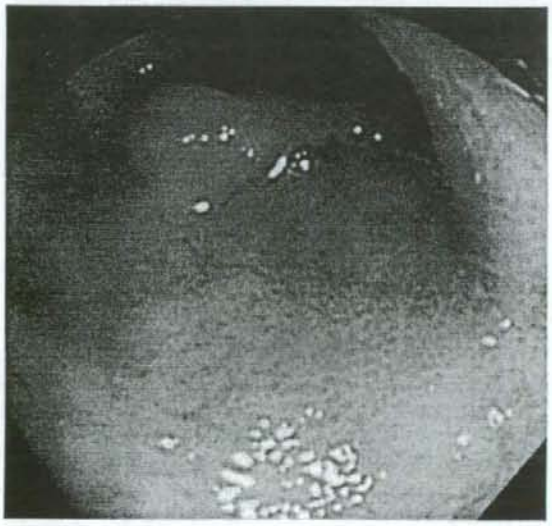

Figure 6　大腸内視鏡検査（4回目）.
経口プレドニゾロン2.5 mgまで減量後.
回腸末端部の下掘れ潰瘍の再発は認めない.

血・穿孔等に最重な注意を払うべきであるとの報告がある[10].

単純性潰瘍の治療法に関しては，確実に有効な薬剤は従来から特に言及されていないが，一般的にはアミノサルチル酸製剤，ステロイド剤が投与されることが多い[5~9]．中心静脈栄養も活動期には腸管安静として積極的に用いられている[10,11]．ベーチェット病に対する免疫抑制剤（アザチオプリン，シクロスポリン，FK-506，抗TNF-αキメラ抗体など）の効果は報告されているが，未だ腸管病変に対する効果は確立されていない[12~16]．本症例においては，入院中に中心静脈栄養およびステロイド投与を行った．ステロイドに関しては，腸管ベーチェット病に対して有効であること，および単純性潰瘍に対しても著効を示すとの報告もあり好んで使用されているが，単純性潰瘍に対するステロイドの効果については未だ不明である[5~7,17]．ステロイドは，急性期の炎症には効果を発揮するものの，潰瘍の縮小治癒効果はないとする報告もある[13]．また，ステロイドの長期投与は腸管穿孔を助長させたり，予後不良の一因となるので慎重な投与が望ましいとされる[18]．本症例においては，通常のステロイド剤であるプレドニゾロン内服や静注にも拘わらず十分な効果は得られなかった．そこで，われわれは回腸末端部潰瘍に対してパルミチン酸デキサメタゾン（リポ化ステロイド）静脈投与を行った.

パルミチン酸デキサメタゾン（リメタゾン®）は，デキサメタゾンをパルミチン酸エステルとして精製ダイズ油に溶解した乳濁性注射剤で，水島らにより日本で初めて開発されたリポ化製剤である[19]．パルミチン酸デキサメタゾンは一種のプロ

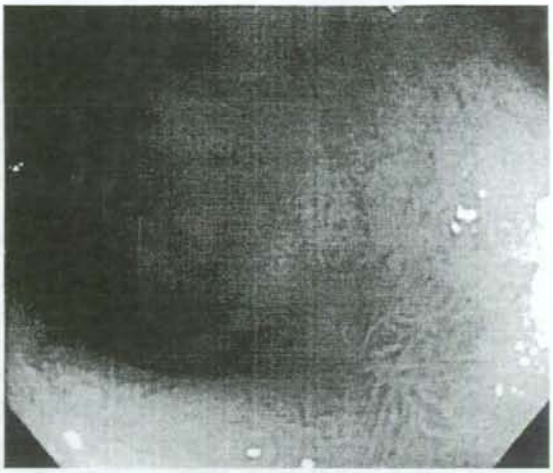

Figure 5　大腸内視鏡検査（3回目）.
パルミチン酸デキサメタゾン（リポ化ステロイド）4.0 mgの静注を計6回施行後回腸末端部の下掘れ潰瘍は，再生上皮が出現し，瘢痕化が認められ著明に軽快改善していた.

ドラックであり，生体内でエラスターゼにより緩徐に加水分解をうけ活性代謝物であるデキサメタゾンになり持続的に抗炎症作用を示す．

したがって，本剤は従来の水溶性デキサメタゾン製剤に比べ投与量の低減化を可能とし，またステロイドに特有な副作用の軽減が期待される抗炎症剤であり，慢性関節リウマチにのみ保険適用となっている．リポ化ステロイドは，ステロイドのみの投与に比べて炎症組織への取り込みが高く抗炎症作用は5～6倍であるといわれているので[19]，単純性潰瘍や腸管ベーチェット病などの炎症性腸疾患における治療法として有効である可能性が示唆されている[20),21)]．本症例のように通常のプレドニゾロン内服や静注では十分な効果が認められない場合やステロイド投与が長期間となる場合には，有効な治療法の1つと考えられる．

IV 結　論

パルミチン酸デキサメタゾン（リポ化ステロイド）静脈投与が有効であった単純性潰瘍の1例を経験した．通常のプレドニゾロン内服や静注では難治性の単純性潰瘍の治療において，パルミチン酸デキサメタゾン（リポ化ステロイド）の静脈投与は選択肢のひとつになり得ると考えられた．

なお，本論文の要旨は第72回日本消化器内視鏡学会総会にて発表した．

文　献

1. 渡辺英伸，遠城寺宗知，八尾恒良．回盲弁近傍の単純性潰瘍の病理．胃と腸 1979；14：749-67.
2. 武藤徹一郎．いわゆる“Simple ulcer”とは．胃と腸 1979；14：739-48.
3. 渡辺　勇，岡田　基，桑原紀之ほか．腸管型Behçet病といわゆるSimple Ulcer—組織学的診断における問題点—．病理と臨床 1984；2：233-44.
4. 渡辺英伸．非腫瘍性腸疾患の病理．病理と臨床 1984；2：1219-30.
5. 飯田三雄，小林広幸，松本主之ほか．腸型Behçet病および単純性潰瘍の経過—X線像の推移を中心として—．胃と腸 1992；28：287-302.
6. 渕上忠彦，長村俊志，堺　勇二．腸型Behçet，単純性潰瘍．胃と腸 1997；32：451-68.
7. 松川正明，山田　聰，荻原達雄ほか．腸型Behçet病・simple ulcerの臨床経過．胃と腸 1992；27：303-11.
8. 多田正大，田中義憲，陶山芳一ほか．再発様式を経過観察しえた回盲部単純性潰瘍の4例．日消誌 1983；80：1636-40.
9. 高橋恒男，武田宏明．特発性小腸潰瘍，腸管ベーチェット．消化器科 1988；13：106-16.
10. 貴島芳彦，山本光成，榎本平之ほか．単純性腸潰瘍5症例の検討．Gastroenterol Endosc 2002；44：780-6.
11. 月岡　忠，鈴木　雄，森　茂紀ほか．栄養療法が奏功した回盲部単純性潰瘍の1例．日消誌 1990；87：1074-7.
12. 安藤　朗，石塚　泉，西山順博ほか．アザチオプリン内服が奏功した腸管型ベーチェット病の1例．Gastroenterol Endosc 2003；45：1056-60.
13. Kaklamani VG, Kaklamanis PG. Treatment of Behçet's disease-an update. Semin Arthritis Rheum 2001；30：299-312.
14. Suzuki N, Kaneko S, Ichino M et al. In vivo mechanisms for the inhibition of T lymphocyte activation by long-term therapy with tacrolimus (FK-506) : experience in patients with Behçet's disease. Arthritis Rheum 1997；40：1157-67.
15. Travis SP, Czajkowski M, McGovern DP et al. Treatment of intestinal Behçet's syndrome with chimeric tumor necrosis factor alpha antibody. Gut 2001；49：725-8.
16. Hassard PV, Binder SW, Nelson V et al. Anti tumor necrosis factor monoclonal antibody therapy for gastrointestinal Behçet's disease : a case report. Gastroenterology 2001；120：995-9.
17. 真武弓子，谷口友章，飯塚文瑛ほか．プレドニンが著効を示した単純性潰瘍（Simple ulcer）の1例．Gastroenterol Endosc 1984；81：1062-5.
18. 西山高志，牧山和也，吉富祐子ほか．腸管ベーチェットが強く疑われた回盲部単純性潰瘍の3例．日本大腸肛門病会誌 1990；43：461-6.
19. Mizushima Y, Hamano T, Yokokawa K. Tissue distribution and anti-inflammatory activity of corticosteroids incorporated in lipid emulsion. Ann Rheum Dis 1982；41：263-7.
20. Yokoyama Y, Suenaga K, Kino J et al. Therapeutic use of a lipid emulsion dexamethasone (dexamethasone palmitate) in inflammatory bowel disease. A new drud delivery system. Jpn Ardh. Int. Med 1995；42：1-7.
21. Hiroshi Nakase, Kazuichi Okazaki, Chiharu Kawanami et al. Therapeutic effects on intestinal Behçet's disease of an intravenous drug delivery system using dexamethasone incorporated in lipid emulsion. J Gastroenterol Hepatol 2001；16：1306-8.

論文受付　平成19年1月29日
同　受理　平成19年9月19日

Inducible expression of microRNA-194 is regulated by HNF-1α during intestinal epithelial cell differentiation

KIMIHIRO HINO,[1,2,3] KIICHIRO TSUCHIYA,[1,3] TARO FUKAO,[1] KOTARO KIGA,[1,2] RYUICHI OKAMOTO,[1] TAKANORI KANAI,[1] and MAMORU WATANABE[1]

[1]Department of Gastroenterology and Hepatology, Graduate School, Tokyo Medical and Dental University, Tokyo 113-8519, Japan
[2]Department of Chemistry and Biotechnology, Graduate School of Engineering, The University of Tokyo, Tokyo, 113-8656, Japan

ABSTRACT

Maintenance of the intestinal epithelium is based on well-balanced molecular mechanisms that confer the stable and continuous supply of specialized epithelial cell lineages from multipotent progenitors. Lineage commitment decisions in the intestinal epithelium system involve multiple regulatory systems that interplay with each other to establish the cellular identities. Here, we demonstrate that the microRNA system could be involved in intestinal epithelial cell differentiation, and that microRNA-194 (miR-194) is highly induced during this process. To investigate this inducible expression mechanism, we identified the genomic structure of the *miR-194-2, -192* gene, one of the inducible class of miR-194 parental genes. Furthermore, we identified its transcriptional regulatory region that contains a consensus-binding motif for hepatocyte nuclear factor-1α (HNF-1α), which is well known as a transcription factor to regulate gene expression in intestinal epithelial cells. By chromatin immunoprecipitation assay and luciferase reporter analysis, we revealed that pri-miR-194-2 expression is controlled by HNF-1α, and its consensus binding region is required for the transcription of pri-miR-194-2 in vivo in an intestinal epithelial cell line, Caco-2. Our observations indicate that microRNA genes could be targets of lineage-specific transcription factors and that microRNAs are regulated by a tissue-specific manner in the intestinal epithelium. Therefore, our work suggests that induced expression of these microRNAs have important roles in intestinal epithelium maturation.

Keywords: microRNA; miR-194; Caco-2; differentiation; HNF-1α; intestine

INTRODUCTION

The intestinal epithelial system is a paradigm for the production of distinct cell lineages from multipotent progenitors (Crosnier et al. 2006). The molecular mechanism of balanced and continuous generation of intestinal epithelial cells has been extensively investigated, as it would be involved in the pathogenesis of gastrointestinal disorders such as intestinal epithelial tumors. Recent studies highlighted the critical roles of specific signaling pathways directing activation of certain transcription factors, such as Notch and Wnt pathways, in the development of intestinal epithelium, clearly indicating that its developmental program is under the control of dynamic gene regulatory networks (Sancho et al. 2004; Fre et al. 2005; Gregorieff and Clevers 2005; Stanger et al. 2005; Clarke 2006; Crosnier et al. 2006).

microRNAs (miRNAs) are 21–23-nucleotide (nt) noncoding RNAs that function as post-transcriptional regulators of gene expression in various species (Ambros 2004; Bartel 2004; Zamore and Haley 2005). miRNAs recognize their target(s) with the partially complementary sequences and repress their translation or modify their stability (Olsen and Ambros 1999; Jing et al. 2005). miRNAs play essential roles in diverse events, including control of developmental timing (Wightman et al. 1993), differentiation (Chen et al. 2004, 2006; Esau et al. 2004; Kim et al. 2006), apoptosis, cell proliferation (Brennecke et al. 2003; Cheng et al. 2005; Cimmino et al. 2005), and organ development (Giraldez et al. 2005).

miRNAs initially appear as relatively long transcripts called pri-miRNA, and it is now widely accepted that many

[5]These authors contributed equally to this work.

Abbreviations: miRNA, microRNA; SI, sucrase-isomaltase; kb, kilobases; LPH, lactase-phlorizin hydrolase; HNF-1α, hepatocyte nuclear factor-1 α; PCR, polymerase chain reaction; RT, reverse transcription; RACE, rapid analysis cDNA end; MEM, minimal essential medium; DMEM, Dulbecco's modified Eagle's Medium; PBS, phosphate buffered saline; FBS, fetal bovine serum.

Reprint requests to: Mamoru Watanabe, Department of Gastroenterology and Hepatology, Graduate School, Tokyo Medical and Dental University, 1-5-45 Yushima, Bunkyo-ku, Tokyo 113-8519, Japan; e-mail: mamoru.gast@tmd.ac.jp; fax: 81-3-5803-0262.

Article published online ahead of print. Article and publication date are at http://www.rnajournal.org/cgi/doi/10.1261/rna.810208.

pri-miRNAs are transcribed by RNA polymerase II (Cai et al. 2004; Lee et al. 2004), suggesting that tissue- and time-specific expression of miRNAs is probably specified at the level of pri-miRNA transcription. Although hundreds of miRNAs were cloned in various species, the regulatory mechanisms of specific pri-miRNAs are still largely unknown. Studies regarding regulation of each pri-miRNA would therefore provide clues to the further understanding of miRNA biology in general or of particular functions in specific cell lineages.

In this study, we focused on the miRNA system as novel molecular machinery in intestinal epithelial cell differentiation. Our high-throughput miRNA expression profiling revealed a dynamic change of the miRNA expression pattern during Caco-2 differentiation, which is one of the most widely known intestinal epithelial differentiation models. In the model, we found that dozens of miRNAs were up- or down-regulated. Among such miRNAs, miR-194 was found to be highly up-regulated with tight tissue specificity. To know the precise regulatory mechanism, we determined the genomic structure of pri-miR-194-2. Given the genomic structure, we also identified a highly conserved genomic region close to the transcription start site of pri-miR-194-2 that contains a consensus binding motif for hepatocyte nuclear factor-1α (HNF-1α). Chromatin immunoprecipitation (ChIP) assay confirmed physical binding of HNF-1α to this conserved region in vivo, and other functional assays further showed the transcriptional role of HNF-1α for the pri-miR-194-2 transcription, suggesting that the conserved genomic region is the core promoter element for pri-miR-194-2 and that HNF-1α is the key transcription factor for the expression of this miRNA.

Because HNF-1α is one of the critical factors of intestinal epithelial gene expression during differentiation and maturation, miR-194 might constitute a certain part of its regulatory network, thereby contributing to the regulation of gene expression program in intestinal epithelial cells. Therefore, our work suggests that induced expression of miRNAs has an important role in intestinal epithelium maturation.

RESULTS

miR-194 is highly induced during intestinal epithelial cell differentiation

Adopting the differentiation system of intestinal epithelial cell line Caco-2, possible alteration of miRNA expression pattern during intestinal epithelial differentiation was examined. Induction of differentiation in Caco-2 cells was performed by conventional long-term confluent culture method. Following confirmation of maturation status by the differentiation markers such as lactase-phlorizin hydrolase (LPH) and sucrase-isomaltase (SI) (Fig. 1A), 156 mature miRNAs were quantified in differentiated and proliferative cells by the TaqMan-based high-throughput profiling method. As shown in Figure 1, B and C, several miRNAs were significantly up- or down-regulated during Caco-2 differentiation as judged by Ct values. Among such genes, expression of miR-133a and miR-133b has been previously detected in tissues other than intestine (Chen et al. 2006). Also, miR-146 has been reported to control Toll-like receptor and cytokine signaling (Taganov et al. 2006), whereas the miR-34 family has been shown to be involved in the p53 network (He et al. 2007). Inhibition of miR-148 and 210 increases the level of apoptosis, while inhibition of miR-152 decreases cell growth (Cheng et al. 2005). Consequently, differentially expressed miRNAs observed in the present experiment suggested that miRNA machineries that control general physiological events are involved in epithelial cell differentiation.

Although identification of sets of miRNA as regulators of general events is important, here, we rather sought to find some miRNAs that are regulated specifically in intestinal epithelial cells. Among differentially expressed miRNAs, miR-194 was one of the highly induced miRNAs during differentiation and showed the highest intensity in differentiated Caco-2 cells (Fig. 1D). Induction of mature miR-194 upon Caco-2 differentiation was also confirmed by Northern blot (Fig. 1E). Also, tissue distribution of mature miRNA-194 in an adult mouse was identified to be relatively specific in intestinal tracts (Fig. 1F), consistent with some previous results in other organisms such as zebrafish embryo (Wienholds et al. 2005).

These data collectively suggested that, among numerous regulated miRNAs, miRNA-194 is highly and specifically induced in intestinal epithelial cells during its differentiation.

Genomic structures of miR-194 primary transcripts

Given the high and specific expression of miR-194 in intestinal epithelial cells, we further sought to characterize this miRNA to know its regulation. According to miRBase, mature miR-194 can be derived from two separate loci on human genome that are registered as *miR-194-1* and *miR-194-2* (Fig. 2A). The miR-194-1 and miR-194-2 are encoded on human chromosomes 1 and 11, respectively. As like many other miRNAs, both miR-194-1 and miR-194-2 are so-called clustered miRNA and have cluster partners miR-215 and miR-192, respectively.

To examine whether either of the two loci can generate mature miR-194, we constructed miRNA expression vectors in which miR-194 loci were inserted downstream of the CMV promoter, and observed mature miR-194 generation using luciferase sensor reporter assay. As luciferase sensor mRNA have perfect complementary sequence against mature miR-194 in 3′UTR, if mature miR-194 is generated from the miR-194 loci, firefly sensor mRNA is cleaved by RNAi effect. Thus, miRNA generation could be observed as reduction of luciferase activity.

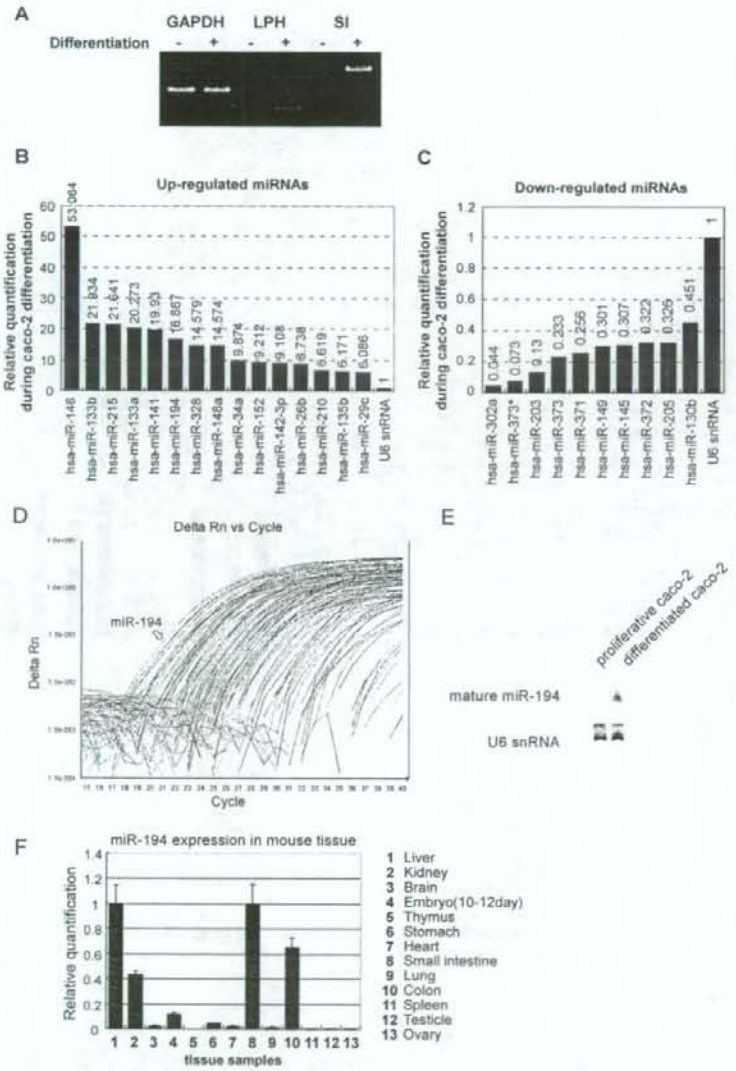

FIGURE 1. Altered expression profile of miRNA during Caco-2 differentiation. (*A*) Detection for differentiation markers by RT-PCR. RT-PCR was performed on total RNAs extracted from proliferative or differentiated Caco-2 cells. PCR products were separated by 5% acrylamide gel electrophoresis and stained by EtBr. (*B*) Up-regulated miRNAs during Caco-2 differentiation. A total of 156 miRNAs were quantified by TaqMan miRNA assays Human Panel–Early Access Kit. Relative Quantification (RQ) was normalized by U6 RNA endogenous control. Quantification results were arranged by RQ and cut-off detectors whose Ct values were more than 30 cycles in differentiated Caco-2 cells. (*C*) Down-regulated miRNAs during Caco-2 differentiation, observed in the quantification performed in *B*. (*D*) Amplification plot by TaqMan miRNA assay in differentiated Caco-2 cells. Arrow indicates amplification plot of miR-194. (*E*) Northern blot of mature miR-194. Total RNAs (30 μg) were separated in 8 M urea 12% PAGE and transferred to Nybond N+. After UV cross-linking, the membrane was hybridized with DIG-labeled RNA probe. Hybridized probes were detected by AP-conjugated anti-DIG antibody and visualized by CDP-star. (*F*) miR-194 expression in various mouse tissues. Expression of miR-194 was quantified by TaqMan miRNA assay. U6 snRNA was used as endogenous control. The expression level in small intestine was set to 1.

Forced expression of each locus showed marked decrease of the sensor luciferase activity in both Hela S3 and Caco-2 cells (Fig. 2B). As the results of this assay showed that both loci are able to generate mature miR-194, we sought to examine which locus is the origin of miR-194 that is induced upon differentiation of intestinal epithelial cells. Northern blot analysis of pre-miRNAs showed up-regulation of both pre-miRNAs (Fig. 2C), whereas TaqMan miRNA assay showed up-regulation of miR-194, miR-192, and miR-215 upon Caco-2 differentiation (Fig. 2D). Quantitative RT-PCR using a reverse-transcribed sample as a standard template also showed induction of pri-miRNA from both loci upon differentiation, but a relatively higher induction of pri-miR-194-2 was observed, compared with pri-miR-194-1 (Fig. 2E, left). Absolute quantification using genomic DNA as a standard template, which enables quantitative comparison between pri-miR-194-1 and pri-miR-194-2, also demonstrated that expression of pri-miR-194-2 was more abundant in differentiated Caco-2 cells, compared with pri-miR-194-1 (Fig. 2E, right).

Having these observations, we focused on miR-194-2 cluster and further characterized this locus. Upon the database search, a registered cDNA, AK092802, was found as a putative 5′ part of the pri-miR-194-2 transcript (Fig. 3A). As shown by RT-PCR, the registered transcript AK092802 and the region encoding pre-miR-194-2 were transcribed primarily as a single RNA (Fig. 3B). Also, the 5′ region of the transcript including the transcription start site of pri-miR-194-2 was determined by 5′ RACE. Although 5′ RACE presented two fragments, sequence analysis revealed that these two fragments arise from the same transcription start site, while the difference in length was due to splicing (Fig. 3C). Furthermore, we performed 3′ RACE to identify the structure of pri-miR-194-2, -192 (Fig. 4A). The identified pri-miRNA shared the same 3′ terminal with that of another registered transcript, AW207381 (Fig. 4B), and induced

expression of the entire transcript was confirmed during Caco-2 cell differentiation (Fig. 4C). Therefore, we examined the genomic structure of pri-miR-194-2 that gives rise to a part of the inducible miR-194 during intestinal epithelial cell differentiation.

Identification of the core promoter element for pri-miR-194-2

To know the transcriptional mechanism, we then sought to analyze the promoter region of pri-miR-194-2. Upstream genomic region close to the transcription start site of pri-miR-194-2 contains several highly conserved regions among human, mouse, rat, and dog (from −162 to +21 with respect to the transcription start site of AK092802) (Fig. 5A). To identify the promoter region, we constructed reporter plasmids carrying various genomic sequences around the transcription start site of pri-miR-194-2 (Fig. 5B) and subjected them to luciferase assay. Results demonstrated that the region from −162 to +21 had a high promoter activity in differentiated Caco-2 cells, comparable to that of the longest region from −1003 to +358 (Fig. 5B). In contrast, deletion of the conserved region dramatically reduced promoter activity.

Since conserved regions in a gene promoter are expected to contain regulatory elements, we focused on such region found within the pri-miR-194-2 promoter. Luciferase assay using a mutated construct revealed that the region from −70 to −52 is critically required for the pri-miR-194-2 promoter activity that is driven by the identified conserved region in differentiated Caco-2 cells, indicating that the corresponding region is the core element of pri-miR-194-2 promoter (Fig. 5C).

HNF-1α regulates pri-miR-194-2 promoter

By a computational search for potential motifs of transcription factors, a putative binding site for HNF-1α was found in the conserved core element of pri-miR-194-2 promoter (Fig. 6A). HNF-1α is a member of a class of transcription factors that is distantly related to homeobox proteins, which contains a DNA binding domain. In addition, HNF-1α has been formerly described as a key transcriptional activator during Caco-2 differentiation (Wu et al. 1994; Mitchelmore et al. 1998; Boudreau et al. 2001, 2002; van Wering et al. 2002). Thus, we hypothesized that HNF-1α might bind to the core element of pri-miR-194-2 promoter and contribute to upregulate pri-miR-194-2 transcription. Indeed, HNF-1α was shown to physically interact to the core element of the pri-miR-194-2 promoter in Caco-2 cells, as judged by ChIP assay (Fig. 6B). Furthermore, forced expression of HNF-1α activated the promoter of both pri-miR-194-2 and SI in HeLa S3 cells, which usually do not express miR-194 (Fig. 6C). Forced expression of HNF-1α in Caco-2 cells also showed an additive effect on the promoter activity of pri-miR-194-2. Mutation in the HNF-1α binding site resulted

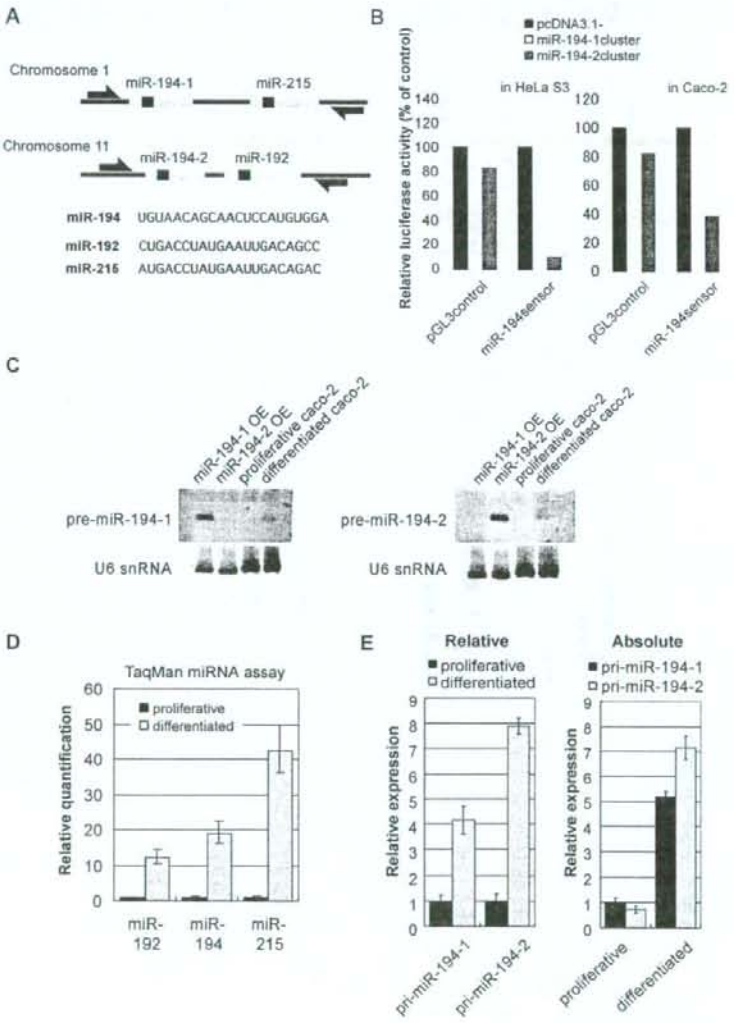

FIGURE 2. (Legend on next page)

in almost complete loss of the pri-miR-194-2 promoter activity, confirming the requirement of HNF-1α binding to the corresponding site for pri-miR-194-2 transcription. Taken together, these data suggest that HNF-1α is a key transcriptional regulator of pri-miR-194-2 and activates its promoter activity by physically binding to the core promoter element.

DISCUSSION

In the present study, we identified the structure of pri-miR-194-2 and determined both transcription start site and 3′ end using 5′ RACE and 3′ RACE, respectively. As pri-miRNAs could be either a protein-coding RNA or a noncoding RNA, we searched in silico for a candidate open reading frame (ORF) within a pri-miR-194-2, -192 transcript and did not find a single protein-coding ORF. In addition, conserved genomic region of pri-miR-194-2, -192 was restricted to the region encoding miRNA hairpin structures. Therefore, we suggest that pri-miR-194-2, -192 is a noncoding RNA.

We also identified that miR-194-2 and miR-192 are encoded within the intron but not in the exon (Fig. 4B). To assure this, we have shown that mature miR-194 surely arises from the miR-194-2, -192 cluster region, a partial sequence of the second intron (Fig. 4B), by forced expression of the corresponding region (Fig. 2B). This means that these miRNAs are processed by splicing and cropping of the pri-miRNA in the nucleus. Indeed, although the PCR product shown in Figure 3B contained the second intron, the PCR product shown in Figure 4C lacked the corresponding intron sequence. This difference may be attributed to the relatively short extension time (1.5 min) used for the PCR in Figure 4C, for detection of the transcript containing the intron (4.8 kb), but also suggests that the second intron containing the miR-194-2, -192 cluster is primarily transcripted along with the three exons but is rapidly spliced out from the pri-miR-194-2.

On the other hand, concerning these processing steps, a model of intronic miRNA processing was recently suggested (Kim and Kim 2007). According to their model, miRNA-harboring intron is detained while other introns are rapidly spliced out. In our study, RT-PCR analysis in Figure 3B showed 2.4-kbp and 1.8-kbp products, which might represent the nascent transcript and the partially spliced transcript for pri-miR-194-2, respectively. As the reverse primer used in the present RT-PCR is placed within the second intron, the result may indicate that the first intron is processed more rapidly, compared with the miRNA-harboring second intron. Therefore, pri-miR-194-2 might be processed through the proposed model.

Also in our study, we demonstrated that miR-194 is highly expressed in differentiated intestinal epithelial cells. Induced expression of miR-194 could be accounted by the regulatory mechanism of *miR-194-2* gene in that a tissue-associated transcription factor, HNF-1α, plays a central role in its transcription. Although HNF-1α is well known for its regulatory roles of various genes specific for the intestine, its expression is not tightly restricted to the intestine but is also found in the liver or the kidney (Mendel and Crabtree 1991). However, mature miR-194 has been reported to appear not only in the intestine but also in the liver and in the kidney (Lagos-Quintana et al. 2003; Krutzfeldt et al. 2005; Wienholds et al. 2005; Kato et al. 2007). Our TaqMan miRNA analyses have also confirmed expression of miR-194 in these tissues (Fig. 1F). These findings are consistent with our present study describing the regulation of miR-194 expression by HNF-1α. Recent studies, however, have highlighted the regulation of mature miRNA generation at the post-transcriptional processing level (Thomson et al. 2006; Viswanathan et al. 2008) Although our data show consistent increase of mature miR-194 upon increase of its pri-miRNAs, there remains a possibility that expression of mature miR-194 might also be regulated at the processing level.

Our promoter analyses revealed that the consensus motif for HNF-1α found within the conserved region of the pri-miR-194-2 promoter plays a critical role in induction of *miR-194-2* gene upon Caco-2 cell differentiation. HNF proteins are known to interact with other transcription factors to regulate the expression of various intestine-specific genes. For example, different members of the HNF family that are expressed in the intestine, such as HNF-1β and

FIGURE 2. Expression of miR-194-2, -192 cluster was induced during Caco-2 differentiation. (*A*) Genomic organization of miR-194 clusters. miR-194-1 and miR-215 are located within an ~400-bp region in chromosome 1. miR-194-2 and miR-192 are located within an ~300-bp region in chromosome 11. Open arrows represent pri-miRNA detection primers used in *E*. (*B*) Both miR-194 loci potentially express mature miR-194. miR-194 expression vector and pGL3miR-194sensor were cotransfected into HeLa S3 cells (*left*) or Caco-2 cells (*right*). As pGL3miR-194sensor contained a sequence completely complementary to mature miR-194 in 3′UTR of luciferase, expression of mature miR-194 is detected by reduced firefly luciferase activity by RNAi. Firefly luciferase reporter activities were normalized by *Renilla* luciferase. The mean value of cells cotransfected with pcDNA3.1 mock vector was set to 100. (*C*) Northern blot of the pre-miR-194s, each arising from distinct loci. Total RNA (30 μg) extracted from proliferative or differentiated Caco-2 cells that were pretreated with Dicer siRNA was analyzed. Positive control (10 μg total RNA) was obtained from Dicer knockdowned 293 cells transfected with miR-194 cluster expression vectors (miR-194-1 OE and miR-194-2, OE, respectively). Probes were designed to hybridize around the loop sequence of each transcript. (*D*) Inducible expression of miRNAs from miR-194 clusters during Caco-2 differentiation. Expression of miR-192, miR-194, and miR-215 were quantified by TaqMan miRNA assay. U6 snRNA was used as endogenous control to normalize expression of miRNAs. The expression level of each miRNA in proliferative Caco-2 cells was set to 1. (*E*) Two distinct miR-194 loci contribute to its induced expression during Caco-2 cell differentiation. RT-PCR was performed with primers indicated in *A*, and GAPDH was used as endogenous control. For relative quantification, expression of each pri-miR-194 within proliferative Caco-2 was used as a standard (*left*). For absolute quantification, genomic DNA was used as a standard. Bar graph is drawn so that pri-miR-194-1 in proliferative Caco-2 cells is set to 1 (*right*).

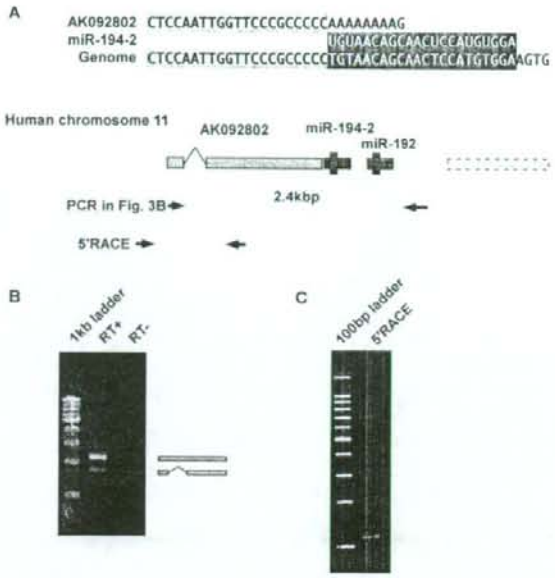

FIGURE 3. Identification of the transcription start site of pri-miR-194-2. (*A*) Genomic sequence and EST information surrounding miR-194-2. 3′ End of AK092802 is adjacent to 5′end of miR-194. Arrow bars represent predicted PCR products. (*B*) AK092802 and miR-194-2, -192 cluster are linked in a single transcript. RT-PCR was performed by total RNA extracted from differentiated Caco-2 cells, using primers indicated in *A*. PCR products were separated by 1% agarose gel electrophoresis and stained by EtBr. Sequence analysis of the amplified products revealed that the 2.4-kbp fragment contained an intronic sequence, while the intronic sequence was spliced out in the 1.8-kbp fragment. (*C*) 5′ RACE analysis of pri-miR-194-2. 5′ RACE was performed using random primers instead of oligo dT primer. PCR was performed by primers indicated in *A*. PCR products were separated by 5% polyacrylamide gel electrophoresis and stained by EtBr. Consistent with *B*, two fragments were observed, and sequence analysis of these fragments revealed that difference was due to an intronic sequence. Both fragments had the same transcription start site.

HNF-4, coordinately enhance target gene expression (Wu et al. 1994; Hu and Perlmutter 1999, 2002; Boudreau et al. 2001). Furthermore, GATA family and caudal related homeobox protein Cdx2 also coordinately enhance expression of intestine-specific genes (Krasinski et al. 2001; Boudreau et al. 2002; Wang et al. 2004). It is therefore speculated that the consensus motif for HNF-1α found within the core promoter region of pri-miR-194-2 may play a pivotal role in different aspects of regulation for this miRNA. Evolutional conservation of this consensus site among phylogenetically distant species further indicates a strong functional link between HNF-1α and miR-194-2 expression and also its significance in essential physiological events.

From the view of environmental regulation of miRNA, a recent study reported that miR-192 ectopically appears in diabetic renal glomeruli and that TGF-β is involved in the induction of this miRNA (Kato et al. 2007). As we have determined in the present study that miR-192 is the clustering partner of miR-194-2, it is possible that TGF-β may also regulate expression of miR-194. Interestingly, it is reported that TGF-β1 can modulate the differentiation process of Caco-2 cells in certain environments (Schroder et al. 1999). Therefore, it is of interest to examine the role of TGF-β upon regulation of miR-194 expression, as this cytokine shows diverse effects on intestinal physiology.

In conclusion, miR-194 is highly induced during intestinal epithelium differentiation, and pri-miR-194-2 expression

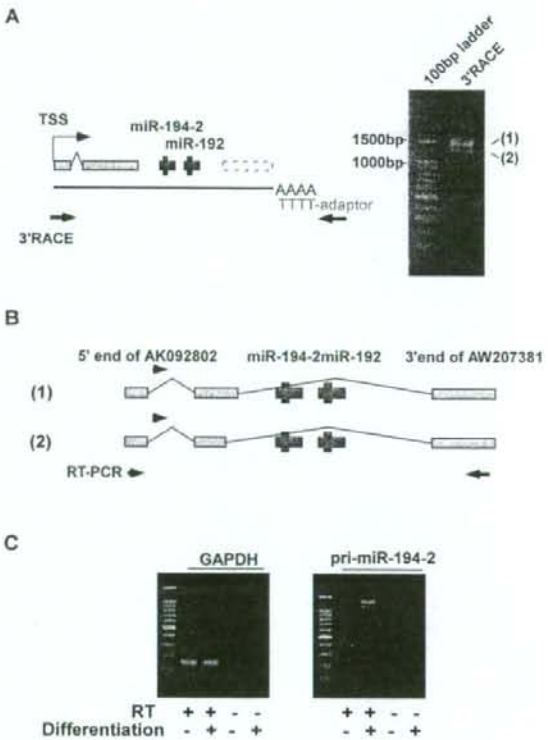

FIGURE 4. Identification of pri-miR-194-2 structure. (*A*) 3′ RACE analysis of pri-miR-194-2. Schematic representation of the primers used in the analysis is shown (*left*). PCR products were separated by 2% agarose gel electrophoresis and stained by EtBr (*right*). Two fragments are shown, designated as 1 and 2. (*B*) Schematic representation of pri-miR-194-2 structures. Sequence analysis revealed that difference in fragments 1 and 2 observed in *A* comes from the difference in length of the second exon. Both fragments had the same 3′ end, which also coincided with the 3′ end of AW207381. (*C*) Induced expression of pri-miR-194-2 during Caco-2 cell differentiation. To confirm the increased expression of the identified pri-miR-194-2 transcript during Caco-2 differentiation, RT-PCR was performed using primers represented in *B*. PCR products were separated by 2% agarose gel electrophoresis, and stained by EtBr.